Redox Biology 70 (2024) 103057

Contents lists available at ScienceDirect

Redox Biology

journal homepage: www.elsevier.com/locate/redox

A natural small molecule aspidosperma-type alkaloid, hecubine, as a new TREM2 activator for alleviating lipopolysaccharide-induced neuroinflammation *in vitro* and *in vivo*

Lin Li [a], Yu-Lin He [a,b], Nan Xu [a], Xiu-Fen Wang [a,d], Bing Song [e,f,g], Ben-Qin Tang [b,c,d,*], Simon Ming-Yuen Lee [a,b,c,**]

[a] *State Key Laboratory of Quality Research in Chinese Medicine and Institute of Chinese Medical Sciences, University of Macau, Macau, China*
[b] *Department of Food Science and Nutrition, The Hong Kong Polytechnic University, Hung Hom, Hong Kong, China*
[c] *Research Centre for Chinese Medicine Innovation, The Hong Kong Polytechnic University, Hung Hom, Hong Kong, China*
[d] *Department of Medical Science, Shunde Polytechnic, Foshan, 528333, China*
[e] *Department of Dermatology, The First Hospital of China Medical University, 110001, Shenyang, China*
[f] *School of Dentistry, Cardiff University, Heath Park, Cardiff, CF14 4XY, UK*
[g] *Institute of Biomedical and Health Engineering, Shenzhen Institute of Advanced Technology, Chinese Academy of Sciences, Shenzhen, China*

A R T I C L E I N F O

Keywords:
TREM2
Aspidosperma-type alkaloids
Hecubine
Microglia
Anti-neuroinflammation
Anti-oxidation

A B S T R A C T

Neuroinflammation and oxidative stress play a crucial role in the pathogenesis of neurodegenerative diseases, including Alzheimer's disease. The triggering receptor expressed on myeloid cells 2 (TREM2), highly expressed by microglia in the central nervous system (CNS), can modulate neuroinflammatory responses. Currently, there are no approved drugs specifically targeting TREM2 for CNS diseases. Aspidosperma alkaloids have shown potential as anti-inflammatory and neuroprotective agents. This study aimed to elucidate the potential therapeutic effect of Hecubine, a natural aspidosperma-type alkaloid, as a TREM2 activator in lipopolysaccharide (LPS)-stimulated neuroinflammation in *in vitro* and *in vivo* models. In this study, molecular docking and cellular thermal shift assay (CTSA) were employed to investigate the interaction between Hecubine and TREM2. Enzyme-linked immunosorbent assay (ELISA), quantitative PCR, immunofluorescence, Western blotting, and shRNA gene knockdown were used to assess the anti-neuroinflammatory and antioxidant effects of Hecubine in microglial cells and zebrafish. Our results revealed that Hecubine directly interacted with TREM2, leading to its activation. Knockdown of TREM2 mRNA expression significantly abolished the anti-inflammatory and antioxidant effects of Hecubine on LPS-stimulated proinflammatory mediators (NO, TNF-α, IL-6, and IL-1β) and oxidative stress in microglia cells. Furthermore, Hecubine upregulated Nrf2 expression levels while downregulating TLR4 signaling expression levels both *in vivo* and *in vitro*. Silencing TREM2 upregulated TLR4 and downregulated Nrf2 signaling pathways, mimicking the effect of Hecubine, further supporting TREM2 as the drug target by which Hecubine inhibits neuroinflammation. In conclusion, this is the first study to identify a small molecule, namely Hecubine directly targeting TREM2 to mediate anti-neuroinflammation and anti-oxidative effects, which serves as a potential therapeutic agent for the treatment of neural inflammation-associated CNS diseases.

Abbreviations: MIAs, Monoterpene indole alkaloids; LPS, Lipopolysaccharide; CNS, central nervous system; TREM2, triggering receptor expressed on myeloid cell-2; TLRs, toll-like receptors; MyD88, myeloid differentiation primary-response protein 88; NF-κB, transcription factor nuclear factor kappa B; ROS, reactive oxygen species; MAPKs, mitogen-activated protein kinase; PI3K, phosphatidylinositol 3-kinase; Nrf2, nuclear factor E2-related factor 2; HO-1, heme oxygenase-1; NO, Nitric oxide; TNF-α, tumor necrosis factor-α; IL-1β, interleukin-1β; IL-6, interleukin-6; IL-10, interleukin-10; iNOS, inducible nitric oxide synthase; AD, Alzheimer's disease; PD, Parkinson's Disease.

* Corresponding author. TU319, Core TU, Department of Food Science and Nutrition, The Hong Kong Polytechnic University, Hung Hom, Hong Kong, China.
** Corresponding author. TU319, Core TU, Department of Food Science and Nutrition, The Hong Kong Polytechnic University, Hung Hom, Hong Kong, China.
E-mail addresses: tangbenqincy@gmail.com (B.-Q. Tang), simon-my.lee@polyu.edu.hk (S.M.-Y. Lee).

https://doi.org/10.1016/j.redox.2024.103057
Received 22 November 2023; Received in revised form 2 January 2024; Accepted 23 January 2024
Available online 24 January 2024

1. Introduction

Neuroinflammation and oxidative stress contribute to a variety of neuropathological diseases and mental health disorders, such as chronic neurodegeneration [1] and drug addiction [2]. Microglia are resident immune cells in the central nervous system (CNS) and play a key role in neuroinflammatory and immune responses [3]. The triggering receptor expressed on myeloid cell-2 (TREM2) is a major endogenous transmembrane receptor highly expressed on microglia that regulates the inflammatory response [4]. TREM2 promotes a switch from a pro-inflammatory M1 microglia to an anti-inflammatory M2 phenotype, resulting in the downregulation of inflammatory cytokines and inhibition of microglial inflammation [5]. Activation of TREM2 and its downstream signaling pathways are pivotal for maintaining microglial homeostasis and promoting neuroprotection in inflammation-associated CNS diseases [6]. In the context of intracerebral hemorrhage (ICH), TREM2 activation can inhibit inflammatory factor production, thereby promoting neuronal cell survival [7]. In an Alzheimer's disease (AD) experimental model, TREM2-deficient microglia fail to effectively encapsulate Aβ plaques, leading to accelerated brain pathology [8]. Contrarily, overexpression of TREM2 *in vivo* and *in vitro* has been shown to promote microglial M2 transformation, decrease the deposition of β-amyloid (Aβ) plaques, and eventually alleviate neuroinflammation [9]. Therefore, all these findings highlight the potential of TREM2 activation as a promising therapeutic target for various neurological disorders. In addition, the vitagene network analysis has identified the targeting of cellular stress responses as a crucial therapeutic approach for inflammation-associated neurodegenerative diseases [10]. The vitagene family encompasses members of the Hsp family, such as heme oxygenase-1 (HO-1) and Hsp72, which can be upregulated by nuclear factor E2-related factor 2 (Nrf2) to initiate multiple protective mechanisms that alleviate oxidative stress [11]. Moreover, the activation of Nrf2-mediated HO-1 expression has been shown to inhibit the activation of microglial cells and prevent the release of inflammatory mediators in AD mice [12].

Lipopolysaccharide (LPS), an agonist of Toll-like receptors (TLRs), acts as an exogenous ligand of TREM2. The activation of TREM2 induced by LPS appears to attenuate the TLR response, resulting in a reduction in the production of pro-inflammatory cytokines [13]. It is reported that TREM2 overexpression mitigated neurological dysfunction induced by ICH in mice by suppressing TLR4 activation, as well as NF-κB and MAPK signaling pathways [14]. Additionally, current research indicates that the activation of TREM2 transcription promotes the upregulation of Nrf2, thereby inhibiting neuroinflammation and alleviating depressive-like behaviors in CSDS mice [15]. Therefore, despite the intricate mechanism of TREM2, there is no doubt that TREM2 is an emerging and promising drug target for the treatment of neuroinflammation and associated neurological disorders. Since no drugs specifically targeting TREM2 have been approved by the FDA yet, a few first-in-class small molecules of TREM2 activators, such as VG-3927 and AL002, are undergoing different phases of clinical trials for neurodegenerative diseases. Thus, there is an urgent need to search for new drug-like small molecules targeting TREM2 to develop new therapeutic agents for the management of neuroinflammation and inflammation-associated CNS diseases.

Monoterpene indole alkaloids (MIAs) are a group of small molecules with a bicyclic structure comprising a benzene ring fused to a five-membered pyrrole ring. To date, over 3000 MIAs have been identified, many of which have therapeutic potential for the treatment of drug addiction, dementia, and pain [16]. Typical MIAs with clinical applications include rhynchophylline (anticonvulsant), brucine (anti--rheumatoid arthritis), quinine (antimalaria), etc [17]. MIAs are a potential source of novel drugs owing to their diverse and unique structures and excellent druggability. *Ervatamia officinalis*, known for its detoxifying properties and its activity to alleviate painful swelling in China and India, has a high abundance of MIAs, including iboga-type alkaloids and aspidosperma-type alkaloids [18]. Intriguingly, iboga-type alkaloids, such as ibogaine, possess psychedelic properties and have been traditionally employed in African religious ceremonies for spiritual purposes [19]. In clinical practice, iboga-type alkaloids are used for the treatment of opioid dependence and various inflammatory conditions [20,21]. Similarly, aspidosperma-type alkaloids in *E. officinalis* have been reported to possess strong anti-inflammatory properties. For instance, Yu Y et al. reported twelve aspidosperma-type dimers, three of which showed good anti-inflammatory effects against microglial activation [22]. Therefore, aspidosperma-type alkaloids in *E. officinalis* represent a valuable source of new anti-inflammatory and neuroprotective medications.

Hecubine, a natural aspidosperma-type MIA found in *E. officinalis*, was initially identified in 1976 [23]. Subsequent research has revealed its potential as a potent anticancer agent, showing activity against a wide range of human tumor cells [24]. However, as the major MIAs in *E. officinalis*, the neuroprotective activities of Hecubine and its mechanism of action remain unclear. In the present study, Hecubine and its structurally similar analogues [mehranine (**1**), lochnericine (**2**), Hecubine (**3**), voafinine (**4**), voaphylline (**5**), voafinidine (**6**), tabersonine (**7**)] were isolated from *E. officinalis*. The anti-neuroinflammatory activities of seven small molecules (compounds **1**–**7**) were evaluated for the first time in BV2 microglia cells. Among them, Hecubine (**3**) was selected as the representative alkaloid for in-depth investigation of its anti-neuroinflammatory effects and mechanism of action in LPS-stimulated neuroinflammation in BV2 microglial cells and zebrafish larvae. Our findings provide the first evidence that Hecubine acts as a TREM2 activator to exert anti-inflammatory and antioxidant effects *in vivo* and *in vitro*. Thus, targeting the activation of TREM2 represents a novel therapeutic strategy for the prevention and treatment of neuroinflammation.

2. Materials and methods

2.1. Materials

An immortalized mouse BV2 microglial cell line was obtained from the Kunming Cell Bank of Type Culture Collection, Kunming Institute of Zoology. LPS (Escherichia coli serotype 055: B5) was obtained from Sigma-Aldrich (St. Louis, MO, USA). Dulbecco's modified Eagle's medium (DMEM), fetal bovine serum (FBS), phosphate-buffered saline (PBS), and penicillin-streptomycin were purchased from Gibco (Gaithersburg, MD, USA). Enzyme-linked immunosorbent assay (ELISA) kits for TNF-α, IL-1β, and IL-10 were purchased from Invitrogen (Carlsbad, CA, USA). Antibodies against inducible iNOS, COX-2, TNF-α, IL-1β, IL-6, p-IKKα/β, IKKα, p-IκBα, IκBα, p–NF–κB (p65), NF-κB (p65), p-AKT, AKT, p38, p-p p38, p44/42, p-p44/42, SAPK/JNK, p-SAPK/JNK, MyD88, Nrf2, HO-1, β-actin, and GAPDH were acquired from Cell Signaling Technology (Beverly, MA, USA); TREM2 was purchased from R & D Systems (Minneapolis, USA); TLR_4 was purchased from Wanleibio (Shenyang, China); Iba1 was purchased from Abcam (Cambridge, UK). HRP-labeled Goat Anti-Rabbit IgG(H + L) and Donkey Anti-Goat IgG(H + L) secondary antibodies were purchased from the Beyotime Institute of Biotechnology (Shanghai, China).

2.2. Microglial cell culture

BV2 cells were supplemented with 10 % heat-inactivated FBS and 1 % PS (v/v) at 37 °C under a 5 % CO_2 atmosphere. Compounds were dissolved in 0.1 % DMSO (v/v, final concentration) and used for cell-based assays. Cells were treated with appropriate concentrations of the compounds for 1 h prior to LPS stimulation (800 ng/ml).

2.3. Zebrafish maintenance

AB wild-type zebrafish were maintained as described in the Zebrafish

Handbook [25]. Briefly, adult zebrafish were maintained at 28.5 °C with a 14 h:10 h light/dark photoperiod. The embryos were raised in embryo medium (0.54 mM KCl, 13.7 mM NaCl, 0.044 mM KH_2PO_4, 0.025 mM Na_2HPO_4, 0.1 mM $MgSO_4$, 0.13 mM $CaCl_2$, and 42 μM $NaHCO_3$; PH 7.4) at a temperature of 28.5 °C. The 4-day post-fertilization (4-dpf) zebrafish larvae were pretreated with Hecubine for 24 h. After that, the larvae were anesthetized with 0.02 % w/v tricaine, and the LPS was micro-injected into the zebrafish brain at 5 dpf. After 24 h, behavioral and biological tests were performed. Ethical approval (UMARE-030-2017) for the animal experiments was granted by the Animal Research Ethics Committee of the University of Macau.

2.4. Survival rate observation

Zebrafish larvae at 4-dpf were exposed to different concentrations of Hecubine for 24 h. The mortality of zebrafish was observed, and survival rates were calculated.

2.5. Locomotion behavioral test

After treatment with Hecubine and LPS, zebrafish larvae at 6 dpf were transferred into a 96-well plate (1 fish/well). Zebrafish locomotion was measured for 30 min using a zebrafish tracking system (Viewpoint Life Sciences, Lyon, France). The total distance traveled by the zebrafish larvae was calculated simultaneously.

2.6. Cell viability

Cell viability was evaluated by the 3-(4,5-dimethylthiazol-2-yl)-2,5-diphenyltetrazolium bromide (MTT; Sigma-Aldrich) reduction assay. In brief, microglia cells were seeded into a 96-well plate (10^4 cells/well) and received the indicated treatments. After that, the cells were incubated with 0.5 mg/ml MTT solution for 3 h. Finally, the absorbance was measured at 540 and 690 nm using a microplate reader (Dynatec MR-7000; Dynatec Laboratories Inc., El Paso, TX, USA).

2.7. Nitrite quantification assay

The BV2 cells were seeded in a 24-well plate at a density of 1.5×10^5 cells per well and incubated overnight. Cells received the indicated treatments, and 50 μl culture medium was then mixed with 100 μl Griess reagent (Biyuntian Biotech, Shanghai, China). Absorbance was measured at 540 nm.

The level of NO of zebrafish larvae was determined by the Griess method, with some modifications. Briefly, after anesthetizing zebrafish with tricaine, the head without the eye and yolk sac regions of larvae (30 larvae per group) were homogenized with ice-cold phosphate buffer (0.1 M, PH 7.4), and then centrifuged (12,000×*g*) at 4 °C for 20 min; the lysates were then collected. Total protein levels were quantified by Bradford's method. Tissue lysate (100 μL) was mixed with 100 μL of Griess reagent and incubated for 15 min at room temperature, and absorbance was then measured at 540 nm.

2.8. Molecular docking

The crystal structure of TREM2 (PDB ID: 5ELI) was downloaded from the Protein Data Bank (https://www.rcsb.org/). The 2D structure of Hecubin was generated by ChemDraw 20.0, then converted to a 3D structure and optimized using Chem3D 20.0. Molecular docking was performed three times using AutoDock Vina (v1.2.3), and the evaluation of the binding degree was based on criteria established in a previous study [26]. After docking, the best binding pose was visualized and analyzed by PyMOL (v2.3.0) and Discovery Studio (v21.1.0).

2.9. Cellular thermal shift assay

After treatment with Hecubine or DMSO for 1 h, BV2 microglia cells were washed and resuspended in ice-cold PBS with cocktail, and transferred to the PCR tubes equally. PCR tubes were heated individually at different temperatures (37, 41, 45, 49, 53, 57, 61, 65, and 69 °C) for 3 min followed by cooling for 3 min at room temperature. The heated lysates were centrifuged at 20,000g for 25 min at 4 °C. Subsequently, the soluble protein was separated from the precipitates and subjected to detection and quantification through Western blotting analysis.

2.10. ELISA assay

Cells were plated, cultured, and treated as described above. After treatment, the culture supernatants were collected. The levels of the inflammatory mediators TNF-α, IL-6, PGE_2, MCP-1, and IL-10 were determined using ELISA kits according to the manufacturer's instructions.

2.11. ROS detection

The intracellular ROS concentration was determined using a dichloro-dihydrofluorescein diacetate (DCFH-DA) probe according to the manufacturer's instructions [27]. Briefly, BV2 cells were incubated with blank DMEM medium containing 10 μM DCFH-DA at 37 °C for 30 min. After that, the cells were washed with PBS and resuspended for flow cytometry analysis.

The production of intracellular ROS of zebrafish larvae was detected using the fluorescent probe CM-H2DCFDA (Sigma-Aldrich). In brief, CM-H2DCFA (15 μM) was added to zebrafish larvae and incubated for 30 min in the dark at 28.5 °C. Then the CM-H2DCFA was washed three times with medium. Larvae were visualized by a Disk Scanning Unit (DSU) Confocal Imaging System (Olympus Co., Tokyo, Japan). Quantitative analysis of ROS was performed using ImageJ (NIH, Bethesda, MD, USA).

2.12. RNA isolation and reverse transcription-polymerase chain reaction (RT-PCR)

Briefly, the total RNA of BV2 cells was extracted using TRIzol reagent (Invitrogen) according to the manufacturer's protocol. RNA was reverse-transcribed to cDNA using SuperScript II Reverse Transcriptase (Invitrogen) with random primers according to the manufacturer's protocol. The qPCR assay was conducted using the SYBR® Premix Ex Taq™ II kit and Mx3005P qPCR system (Agilent Technologies, Santa Clara, CA, USA). Each sample was normalized to the *β-actin* levels. The primer sequences of each gene are listed in Table 1.

For zebrafish samples, the larvae were anesthetized with 0.02 % w/v tricaine, and the head portion of larvae without the eye and yolk sac regions (30 larvae per group) was collected, and the total RNA of these zebrafish tissues was extracted using TRIzol reagent (Invitrogen)

Table 1
Primers of cell samples used for quantitative RT-PCR.

iNOS- Forward	CAAGAGTTTGACCAGAGGACC
iNOS- Reverse	TGGAACCACTCGTACTTGGGA
COX-2- Forward	TTGAAGACCAGGAGTACAGC
COX-2- Reverse	GGTACAGTTCCATGACATCG
TNF-α- Forward	CCTATGTCTCAGCCTCTTCT
TNF-α- Reverse	CCTGGTATGAGATAGCAAAT
IL-1β- Forward	GGCAACTGTTCCTGAACTCAACTG
IL-1β- Reverse	CCATTGAGGTGGAGAGCTTTCAGC
IL-6- Forward	CCACTTCACAAGTCGGAGGCTT
IL-6- Reverse	CCAGCTTATCTGTTAGGAGA
β-actin- Forward	ATCCTGA AAGACCTCTATGC
β-actin- Reverse	AACGCAGCTCAGTAACAGTC

following the manufacturer's protocol. The rest of the steps were performed as described above. The abundance of mRNA was normalized to the elongation factor 1 α (*ef1a*) levels. The primer sequences of each gene are listed in Table 2.

2.13. Western blot analysis

Cells were lysed with RIPA buffer containing 1 % saturated PMSF and 1 % protease and phosphatase inhibitor cocktail. Protein concentrations were measured using the Bradford Protein Assay Kit (ThermoFisher Scientific, Waltham, MA, USA). Aliquots of protein samples were separated by 10 % SDS-PAGE, transferred to polyvinylidene difluoride (PVDF) membranes, blocked with 5 % non-fat milk, and incubated with specific primary antibodies overnight at 4 °C. After washing, membranes were incubated with HRP-linked secondary antibody for 1 h. Finally, proteins were visualized using an ECL advanced Western blotting detection kit. Photos of the protein bands were taken using Image Lab (Bio-Rad, Hercules, CA, USA). Densitometry measurements of band intensity were determined using ImageJ.

For zebrafish samples, the larvae were anesthetized with 0.02 % w/v tricaine, and the head portion of the larvae without the eye and yolk sac regions (30 larvae per group) were collected, and the protein was extracted using RIPA buffer containing protease phosphatase inhibitor, followed by centrifugation (13,000×*g*) for 15 min at 4 °C. The supernatants were collected, and protein concentrations were measured. The rest of the steps were conducted as described above.

2.14. Immunofluorescence assay

In brief, cells were washed, fixed, permeabilized, and blocked. After that, the cells were sequentially incubated with rabbit anti-p65 antibody (1: 500; Cell Signaling Technology) at 4 °C overnight. Then, cells were incubated with secondary antibodies and DAPI at room temperature. Finally, the samples were imaged using the DMi8 inverted fluorescent microscope (Leica Microsystems, Wetzlar, Germany).

2.15. siRNA, shRNA, and transfection

In this experiment, siRNA targeted at Nrf2 (Santa Cruz Biotechnology, Santa Cruz, CA, USA) was used to knock out the Nrf2 gene. A lentiviral vector expressing mouse TREM2-shRNA was constructed by IGEBIO (Guangzhou, China). The shRNA targeting TREM2 had the sequence 5′-GGAATCAAGAGACCTCCTTCC-3'. The scrambled RNA sequence, used as a control, had the sequence 5′-TTCTCCGAACGTGTCACGT-3'. Briefly, siRNA or shRNA were transfected into BV2 microglia cells that were cultured until 60–70 % confluent using Lipofectamine® 8000 reagent (Invitrogen) in accordance with the manufacturer's protocol. Further experiments were performed at 24 or 36 h after transfection.

2.16. Data and statistical analysis

Each experiment was repeated at least three times independently. Data were analyzed using GraphPad Prism 8.3.0 software (GraphPad Software Inc., San Diego, CA, USA), and are presented as mean ± SD or mean ± SEM. The normality assumption of the data was assessed using the Shapiro-Wilk test or the D'Agostino-Pearson omnibus test, and the assumption of equal variances was evaluated using the Brown-Forsythe test. Nonparametric tests (for non-normally distributed variables) with Kruskal-Wallis tests or one-way ANOVA (for three or more groups of normally distributed variables) with post-hoc Dunnett's tests were used for all statistical analyses. $*/^{\#}p < 0.05$, $**/^{\#\#}p < 0.01$, and $***/^{\#\#\#}p < 0.001$ were considered statistically significant.

Table 2
Primers of zebrafish samples used for quantitative RT-PCR.

iNOS- Forward	GGAGATGCAAGGTCAGCTTC
iNOS- Reverse	GGCAAAGCTCAGTGACTTCC
TNF-α- Forward	gCTggATCTTCAAAgTCgggTgTA
TNF-α- Reverse	TgTgAgTCTCAgCACACTTCCATC
IL-1β- Forward	CATTTgCAggCCgTCACA
IL-1β- Reverse	ggACATgCTgAAgCgCACTT
IL-6- Forward	TCAACTTCTCCAgCgTgATg
IL-6- Reverse	TCTTTCCCTCTTTTCCTCCTg
ef1α- Forward	GCTCAAACATGGGCTGGTTC
ef1α- Reverse	AGGGCATCAAGAAGAGTAGTACCG

3. Results

3.1. Hecubine and its analogues isolated from E. officinalis inhibited LPS-induced NO production in BV-2 microglia cells

The chemical structures of Hecubine (compound **3**) and its structurally similar analogues (compounds **1–7**) (Fig. 1) isolated from *E. officinalis* were identified using NMR and MS analysis (Figs. S1–4). In this study, we evaluated the anti-neuroinflammatory activities of compounds **1–7** by measuring NO production. The results indicated that compounds **1**, **3** (Hecubine), and **4** showed the least toxicity towards microglia BV2 cells. The NO assay results revealed that compounds **1**–**7** exhibited different degrees of potent inhibitory activities against LPS-induced NO production in BV2 microglial cells. Notably, the NO level in LPS-induced microglia treated with 25 μM of Dexamethasone (Dex), the positive control drug, was reduced by 71.1 %. Similar to Dex, compounds **1** and **3** (Hecubine) showed the highest activities, achieving 62 % and 73 % NO inhibition rates at a concentration of 25 μM, respectively. Thus, compound **3** (Hecubine) exhibited the strongest NO production inhibitory effect. Hecubine (compound **3**) was selected for further study of biological activities and underlying mechanisms of action (Table 3).

3.2. Hecubine directly binds to TREM2 to inhibit neuroinflammation

As increasing evidence indicates TREM2 is involved in the pathophysiology of neuroinflammation, we further explored the role of TREM2 underlying the anti-neuroinflammatory effect of Hecubine. An *in silico* molecular docking experiment was performed to explore the possible binding between Hecubine and the TREM2 protein. Interestingly, a strong binding activity (affinity: 7.07 ± 0.03 kcal/mol) was obtained, and Hecubine targeted TREM2 by forming carbon hydrogen bonds with the amino groups of ASP87, ASP86, and PHE74 (Fig. 2a). The Hecubine-TREM2 binding was further confirmed by the cellular thermal shift assay (CETSA) in BV2 cells, which detects changes in protein melting curves caused by drug binding and indicates a shift in the protein's melting temperature (Tm) [28]. CETSA results showed that the addition of 25 μM Hecubine markedly increased TREM2 accumulation at temperatures ranging from 37 °C to 69 °C (relative to the DMSO solvent control), and the Tm value of TREM2 shifted by 6.4 ± 0.7 °C, indicating a direct interaction between Hecubine and TREM2 (Fig. 2b). To further elucidate the role of TREM2 in this process, the expression of TREM2 was knocked down by transfection with TREM2 shRNA (Fig. 2c). RT-PCR analysis revealed that TREM2 knockdown abolished the inhibitory effects of Hecubine on LPS-activated mRNA expression levels of TNF-α and IL-1β (Fig. 2d). These results further support the notion that TREM2 is a potential drug target of Hecubine in anti-neuroinflammation.

3.3. Hecubine inhibited the expression of NO/iNOS and PGE_2/COX-2, and modulated the release of inflammatory factors in LPS-activated BV2 microglial cells

We further investigated the anti-inflammatory effect of Hecubine in BV2 cells. The MTT assay demonstrated that Hecubine (12–25 μM) did

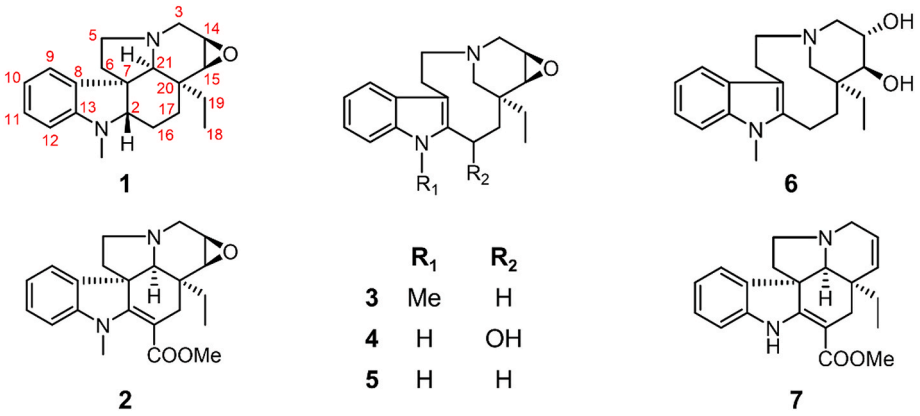

Fig. 1. Chemical structures of Hecubine and its analogues (compounds **1–7**).

Table 3
Inhibitory effects of Hecubine and its analogues (compounds **1–7**) isolated from *E. officinalis* on LPS-induced NO release of BV2 microglial cells.

Compound	Cell viability	NO Inhibition (% of LPS)							
	IC_{50} (μM)	Normal control (Cells only)	LPS/drugs (0.7 μM)	LPS/drugs (1.5 μM)	LPS/drugs (3 μM)	LPS/drugs (6 μM)	LPS/drugs (12 μM)	LPS/drugs (25 μM)	LPS/drugs (50 μM)
1	≫100	94.3 ± 0.7	(−)	(−)	(−)	(−)	(−)	61.8 ± 4.0 ***	75.7 ± 1.9 ***
2	28.7 ± 1.2	97.4 ± 0.4	11.2 ± 2.0 *	31.3 ± 3.2 ***	(−)	(−)	(−)	(−)	(−)
3 (Hecubine)	73.1 ± 1.9	96.6 ± 0.4	(−)	(−)	(−)	52.1 ± 0.1 ***	64.6 ± 0.1 ***	73.8 ± 0.1***	(−)
4	≫100	96.6 ± 0.4	(−)	(−)	(−)	(−)	41.1 ± 0.8 **	50.0 ± 4.7 ***	64.2 ± 5.4 ***
5	56.7 ± 1.8	90.9 ± 1.6	(−)	(−)	39.6 ± 5.4 ***	50.5 ± 3.5 ***	65.3 ± 2.1 ***	(−)	(−)
6	56.7 ± 1.9	92.3 ± 0.2	(−)	37.8 ± 4.7 ***	44.4 ± 4.7 ***	54.1 ± 4.3 ***	(−)	(−)	(−)
7	16.1 ± 1.1	90.7 ± 1.8	18.8 ± 7.0 *	29.3 ± 3.1 **	45.9 ± 2.4 ***	(−)	(−)	(−)	(−)
Dexamethasone	≫100	97.3 ± 0.6	(−)	(−)	(−)	(−)	61.9 ± 4.7	71.1 ± 3.0	75.1 ± 1.9

BV2 cells were stimulated with LPS (800 ng/ml) for 24 h after pretreatment with different concentrations of compounds **1–7** or Dexamethasone for 1 h. Cell supernatants were collected and assayed for NO production using the Griess reaction assay. Each value represents the mean ± SD of three experiments. (−) represents undetermined. *$p < 0.05$, **$p < 0.01$, and ***$p < 0.001$ vs. LPS group.

not exhibit any cytotoxic effects on BV2 cells (Fig. 3b). Subsequently, we treated BV2 microglial cells with Hecubine at concentrations of 6, 12, and 25 μM to assess its effects on NO and PGE2 production as well as the expression of iNOS and COX-2 in LPS-stimulated cells. LPS significantly increased the production of NO and PGE_2, while pretreatment with Hecubine for 1 h dose-dependently reduced the LPS-induced production of NO and PGE_2. Notably, 25 μM Hecubine effectively reduced the PGE_2 production to 15.3 % of that of the LPS-treated group (Fig. 3c and d). Moreover, pretreatment with Hecubine markedly suppressed LPS-mediated increases in protein expression levels of iNOS and COX-2, which are pro-inflammatory mediators of NO and PGE_2 generation, respectively (Fig. 3e and f). Correspondingly, Hecubine also markedly suppressed the upregulation of iNOS and COX-2 mRNA expression induced by LPS stimulation (Fig. 3g and h).

We then investigated the effects of Hecubine on inflammatory cytokine release in LPS-activated BV2 microglial cells. As illustrated in Fig. 4, the LPS-induced increases in TNF-α (Fig. 4a), IL-6 (Fig. 4b), IL-1β (Fig. 4c), and MCP-1 (Fig. 4d) secretions were significantly suppressed by Hecubine treatment. Moreover, Hecubine also markedly suppressed the protein expression of TNF-α and IL-1β in LPS-activated BV-2 microglia (Fig. 4f–h). Interestingly, the maximum inhibitory effect on IL-6 production was achieved by 25 μM Hecubine, where the levels of IL-6 decreased to <8.8 % of that in the LPS-treated group, similar to the control group. Additionally, the production of the anti-inflammatory cytokine IL-10 markedly decreased upon LPS stimulation, while Hecubine pretreatment reversed this trend in a dose-dependent fashion (Fig. 4e). Therefore, Hecubine can down-regulate pro-inflammatory cytokines and up-regulate anti-inflammatory cytokines, thereby suppressing the LPS-induced inflammatory response.

3.4. Hecubine prevented the LPS-induced activation of the TLR4 pathway via activating TREM2 signaling

We initially examined the levels of two important regulators, TLR4 and TREM2, in LPS-treated BV2 cells, as the imbalance of TLR4 and TREM2 intensifies inflammation in BV2 cells [29]. The Western blot showed Hecubine pretreatment effectively increased TREM2 expression in a dose-dependent manner but inhibited TLR4 and MyD88 expressions, which were upregulated by LPS in BV2 cells (Fig. 5a–c). Furthermore, TREM2-shRNA could block the inhibitory effects of Hecubine on the expression of TLR4 (Fig. 5d). Besides, we assessed the expression levels of MAPKs and the PI3K/Akt signaling pathway in BV2 microglial cells, which are regulated by TLR4 signaling. The result revealed that Hecubine obviously suppressed LPS-induced phosphorylation of p38 (Fig. 5e), JNK (Fig. 5f), ERK 1/2 (Fig. 5g), and AKT (Fig. 5h). Notably, 25 μM Hecubine markedly inhibited the phosphorylation of p38 and AKT to ~55 % and ~54.4 % of those of the LPS-treated group, respectively.

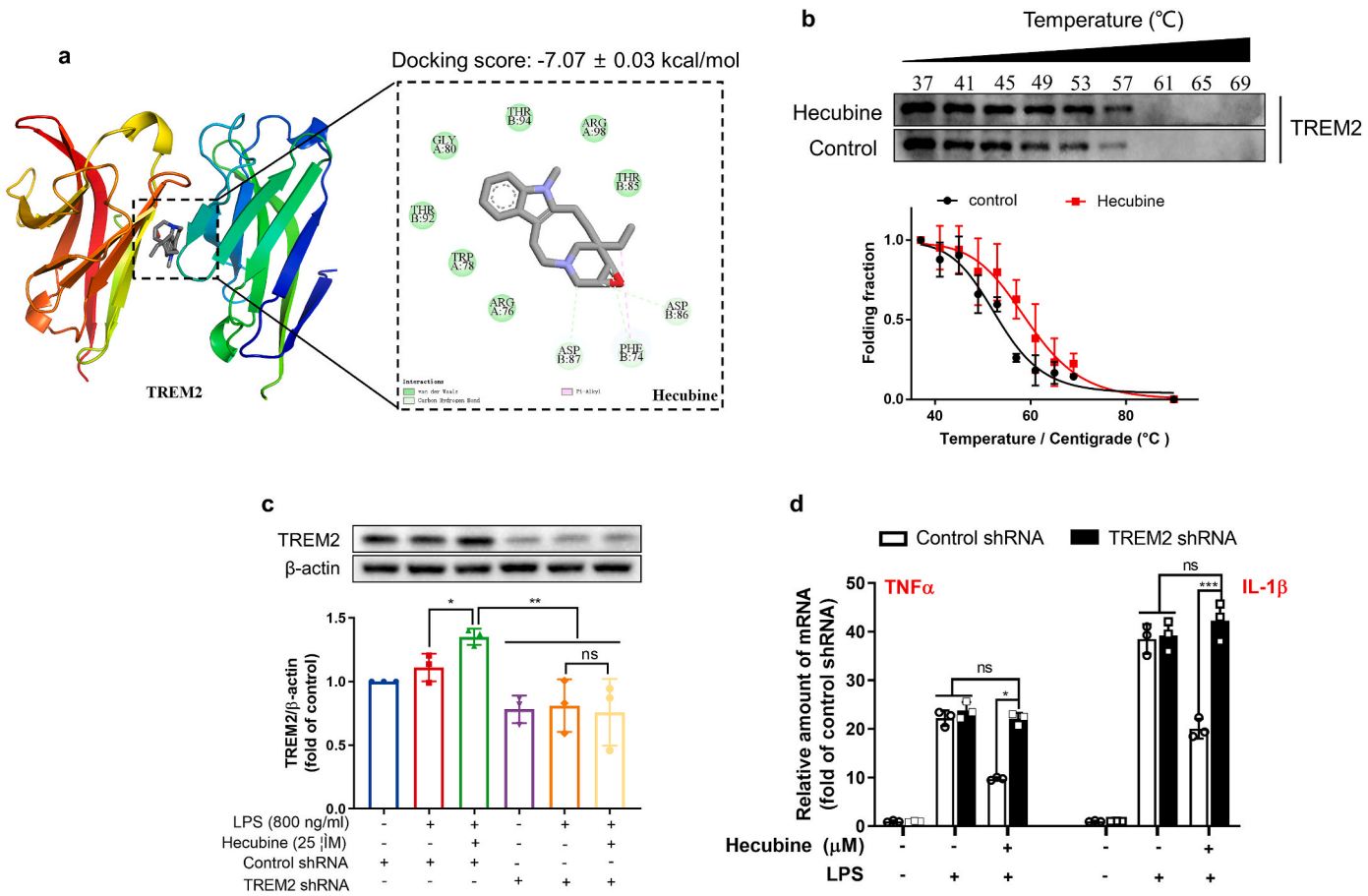

Fig. 2. Hecubine directly binds to TREM2. (a) The interaction of Hecubine with the TREM2 protein in molecular docking analysis. (b) The CETSA assay determined the thermal stabilization of TREM2 interaction with Hecubine at a series of temperatures from 37 °C to 69 °C under a short drug exposure (1 h). (c) Western blot analysis of TREM2 knockdown in BV2 cells. Cells were transfected with negative control shRNA or TREM2 shRNA. n = 3; two-way ANOVA with Dunnett's multiple comparisons test. (d) qPCR analysis of TNF-α and IL-1β in BV2 cells transfected with TREM2 shRNA. n = 3; two-way ANOVA with Dunnett's multiple comparisons test. The data are presented as the mean ± SD of three independent experiments. *$p < 0.05$, **$p < 0.01$, and ***$p < 0.001$ vs. LPS-treated group; ns, not significant.

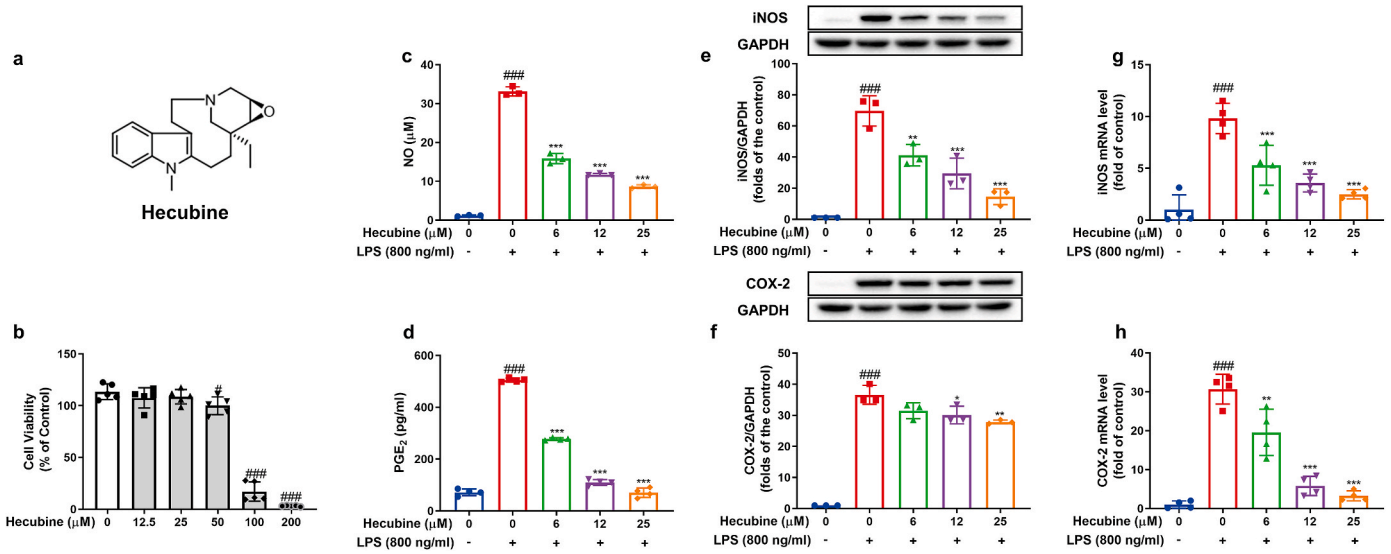

Fig. 3. Hecubine blocked the NO/iNOS and PGE_2/COX-2 pathways in LPS-activated BV-2 microglial cells. (a) Chemical structure of Hecubine. (b) The cell viability of Hecubine with respect to BV2 cells was determined using the MTT assay (n = 5). (c, d) Cells were treated with different doses of Hecubine (0–200 μM) for 24 h. NO levels in the cell culture medium were detected by Griess assay (c), and PGE_2 production was determined by ELISA (c, n = 3; d, n = 4) (d). (e, f) Protein levels of iNOS and COX-2 were measured by Western blot analysis (n = 3). (g, h) The mRNA levels of iNOS and COX-2 were detected by RT-PCR analysis (n = 4). – and + represent the absence and presence of LPS (800 ng/ml), respectively. The data are presented as the mean ± SD of three independent experiments. *$p < 0.05$, **$p < 0.01$, and ***$p < 0.001$ vs. LPS-treated group; #$p < 0.05$ and ###$p < 0.001$ vs. control; One-way ANOVA with Dunnett's multiple comparisons test.

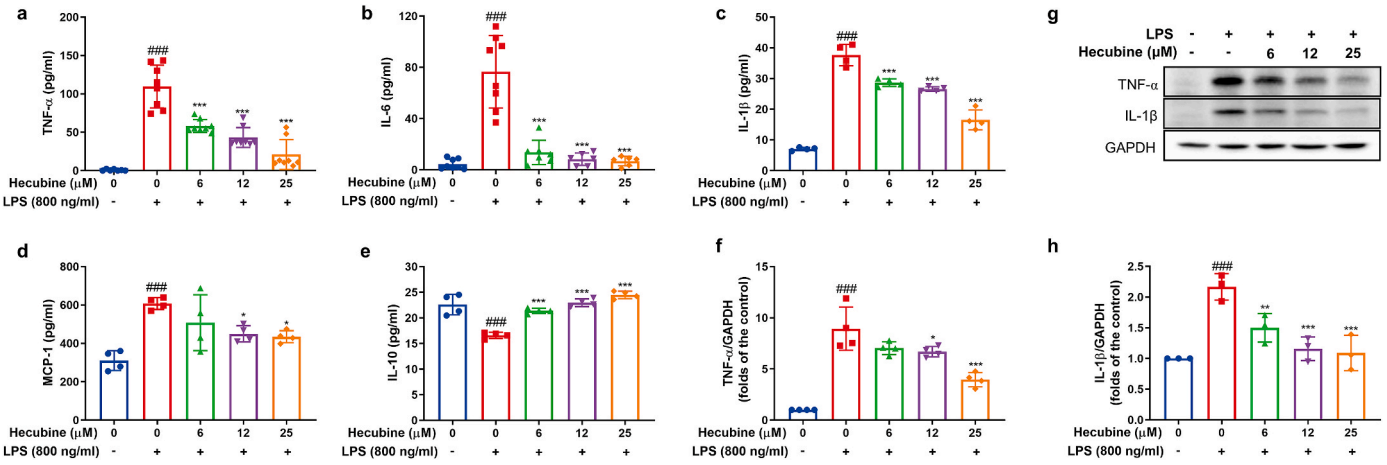

Fig. 4. Hecubine affected the secretion and protein levels of inflammatory cytokines in LPS-stimulated BV-2 cells. Cells were pretreated with Hecubine for 1 h and then exposed to LPS for another 24 h. The production of TNF-α, n = 8 (a), IL-6, n = 6–8 (b), IL-1β, n = 4 (c), MCP-1, n = 4 (d), and IL-10, n = 4 (e) in the cell culture medium was determined by ELISA. (f–h) The protein expression levels of TNF-α (n = 4) and IL-1β (n = 3) were measured by Western blot analysis. – and + represent the absence and presence of LPS (800 ng/ml), respectively. The data are presented as the mean ± SD of three independent experiments. $*p < 0.05$, $**p < 0.01$, and $***p < 0.001$ vs. LPS-treated group; $###p < 0.001$ vs. control; One-way ANOVA with Dunnett's multiple comparisons test.

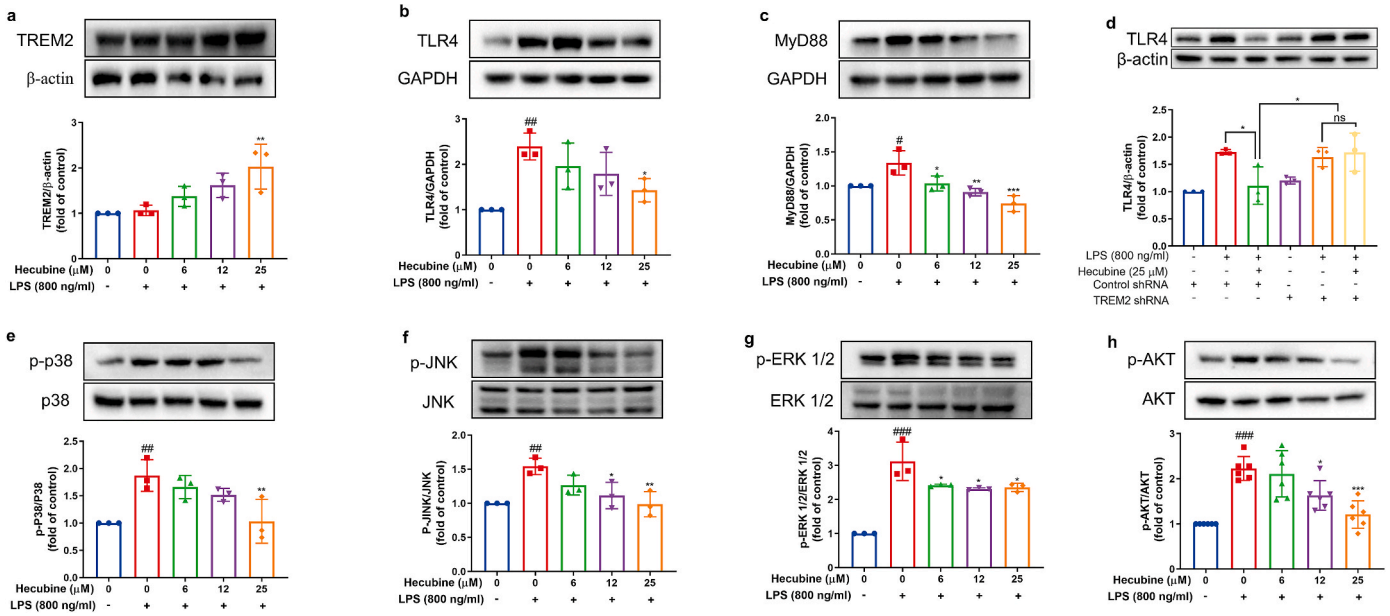

Fig. 5. Hecubine abrogated the LPS-induced imbalance of TREM2 and TLR4 by down-regulating MAPK and PI3K/AKT signaling pathways in LPS-activated BV2 microglial cells. Cells were pretreated with Hecubine for 1 h and then stimulated with/without LPS. After that, the protein levels of TREM2 (Kruskal-Wallis test of One-way ANOVA) (a), TLR4 (Kruskal-Wallis test of One-way ANOVA) (b), MyD88 (c), the total and phosphorylated p38 MAPK (e), JNK (f), ERK 1/2 (g), and AKT (h) levels, were determined by Western blotting (a-g, n = 3; h, n = 6). (d) Cells were transfected with negative control shRNA or TREM2 shRNA, and then TLR4 expression level in BV2 cells after treatment with Hecubine or LPS was assessed by Western blot analysis. Quantitative analysis was carried out using ImageJ. – and + represent the absence and presence of LPS (800 ng/ml), respectively. The data are presented as the mean ± SD of three independent experiments. $*p < 0.05$, $**p < 0.01$, and $***p < 0.001$ vs. LPS-treated group; $###p < 0.001$ vs. control; ns, not significant; One-way ANOVA with Dunnett's multiple comparisons test.

3.5. Hecubine suppressed the activation of the NF-κB pathway in LPS-activated BV-2 microglial cells

As the downstream signaling of MAPKs and the PI3K/AKT pathway, NF-κB signaling plays an essential function in the transcriptional regulation of the expression of several pro-inflammatory mediators. We investigated the effect of Hecubine on the activation of the NF-κB pathway in LPS-activated BV-2 microglial cells. The results showed that exposure to LPS promoted the phosphorylation of IKKα/β, IκB α, and P65 in microglia BV-2 cells, whereas pretreatment with Hecubine obviously inhibited p-IKKα/β, p-IκB α, and p-P65 expression compared with the LPS stimulation group (Fig. 6a–d). Moreover, the effects of Hecubine on the nuclear translocation of the NF-kB p65 subunit were explored. We found that, after LPS treatment for 2 h, the nuclear levels of P65 were markedly increased, while the cytoplasmic levels were remarkably decreased (Fig. S5). After treatment with LPS for 2 h, Hecubine pretreatment significantly reduced the LPS-activated nuclear translocation of NF-κB p65 to ~59.9 % of that of the LPS-treated group (Fig. 6e and f). Moreover, immunofluorescence analysis revealed that Hecubine (25 μM) significantly alleviated the LPS-stimulated accumulation of NF-kB p65 in the nuclei (Fig. 6g). These results indicated that Hecubine might be a potent inhibitor of the activation and translocation of NF-κB p65 in LPS-induced BV2 microglial cells.

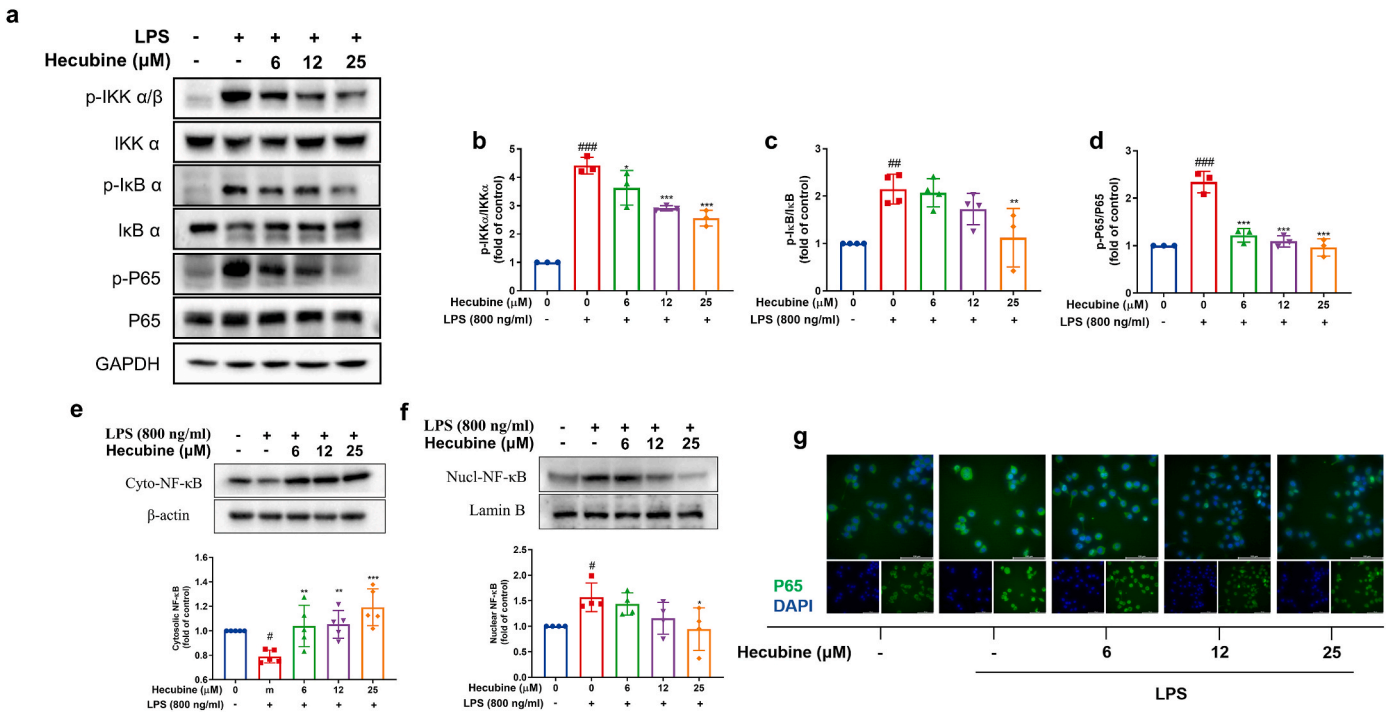

Fig. 6. Hecubine suppressed LPS-triggered activation of the NF-κB p65 pathway in BV-2 cells. Cells were pretreated with Hecubine for 1 h and then stimulated with/without LPS. (a–d) The levels of total/phosphorylated IKKα/β (b), IκB α (c), and P65 (d) were measured via Western blot (b, n = 3; c, n = 4; d, n = 3). (e–f) The expression levels of total NF-κB p65 in the cytoplasmic fraction (n = 5) (e) and nuclear fraction (n = 4) (f) were quantified by Western blot. (g) The nuclear translocation of p65 was evaluated by immunofluorescence analysis. Cells were stained with anti-p65 antibody (green) and DAPI (blue). – and + represent the absence and presence of LPS (800 ng/ml), respectively. The data are presented as the mean ± SD of three independent experiments. *$p < 0.05$, **$p < 0.01$, and ***$p < 0.001$ vs. LPS-treated group; ###$p < 0.001$ vs. control; One-way ANOVA with Dunnett's multiple comparisons test. (For interpretation of the references to colour in this figure legend, the reader is referred to the Web version of this article.)

3.6. Hecubine prevented ROS production but enhanced Nrf2 and HO-1 expression through TREM2 activation in LPS-activated BV2 cells

Intracellular ROS can modulate inflammation through the Akt-mediated activation of NF-κB [30]. Hence, the effect of Hecubine on LPS-induced ROS production was explored. Flow cytometry analysis revealed that LPS treatment obviously elevated the production of ROS, but this was prevented by Hecubine (Fig. 7a). Additionally, Hecubine increased the protein expression of Nrf2 and HO-1 in LPS-stimulated BV2 cells by 4.45 and 8.69-fold at 25 μM, respectively (Fig. 7b). Moreover, treatment with Hecubine alone also significantly increased the expression of Nrf2 and HO-1 in a dose-dependent fashion (Fig. 7c). Furthermore, knockdown of TREM2 decreased the expression of Nrf2 compared to the negative control shRNA group, whereas knockdown of TREM2 did not inhibit the uptrend of Nrf2 after treatment with Hecubine (Fig. 7d).

3.7. Blockade of Nrf2 abolished the inhibitory and anti-inflammatory effects of Hecubine

To further explore whether the Nrf2 pathway is involved in the anti-inflammatory effect of Hecubine, Nrf2 knockdown was achieved via Nrf2 siRNA and control siRNA transfection in BV2 cells. The results indicated that Hecubine significantly increased the protein expression levels of Nrf2 and HO-1 in the control siRNA group, whereas this effect was largely abolished by Nrf2 siRNA transfection (Fig. 8a and b). In addition, the expression levels of TLR4 and MyD88 were measured after treatment with Nrf2 siRNA. As expected, we found that the inhibitory effects of Hecubine on TLR4 and MyD88 expression were abolished in Nrf2 siRNA-transfection BV2 cells (Fig. 8c). Furthermore, Nrf2 knockdown significantly abrogated the Hecubine-mediated inhibition of NO, TNF-α, and IL-6 production (Fig. 8d). Correspondingly, compared with the Hecubine group, the Nrf2 siRNA group displayed higher mRNA expression levels of iNOS, TNF-α, IL-1β, and IL-6 (Fig. 8e). Moreover, no significant differences were observed between the Nrf2 siRNA-LPS + Hecubine group and the Nrf2 siRNA-LPS alone group (Fig. 8f). However, the anti-inflammatory effect of Hecubine on BV-2 microglia did not specifically target Nrf2 in the CETSA assay (Fig. S6). Nonetheless, these results suggest that Nrf2 plays a crucial role in inflammation in LPS-stimulated BV2 cells.

3.8. Hecubine alleviated locomotion behavior deficits and prevented microglia activation and pro-inflammatory cytokine production in a neuroinflammation model of LPS-stimulated zebrafish larvae

In this study, zebrafish larvae were pretreated with Hecubine at 4 dpf for 24 h; LPS was then specifically injected into the heads of zebrafish larvae using our recently developed neuroinflammation zebrafish model (Fig. 9a) [31]. The acute toxicity result showed that Hecubine had no significant impact on the survival rate of zebrafish larvae in 4 dpf at a concentration of ≤25 μM (Fig. 9b). Additionally, 2.5 mg/ml of LPS markedly decreased the total swimming distance (Fig. S7), while treatment with Hecubine (6, 12, and 25 μM) significantly increased the swimming distance of zebrafish, suggesting that Hecubine can restore locomotory behavioral deficits in zebrafish larvae induced by LPS (Fig. 9c).

Following this, the NO level in the zebrafish model was determined. LPS treatment resulted in a ~1.5-fold increase in NO production compared to the control group. However, the increase in NO level was significantly suppressed by pretreatment with Hecubine (25 μM) (Fig. 9d). Subsequently, the protein level of Iba1 was assessed to evaluate microglial cell activation in zebrafish. As expected, Hecubine (25 μM) obviously suppressed the protein expression of Ibal in LPS-activated zebrafish (Fig. 9e). Correspondingly, we investigated the effects of

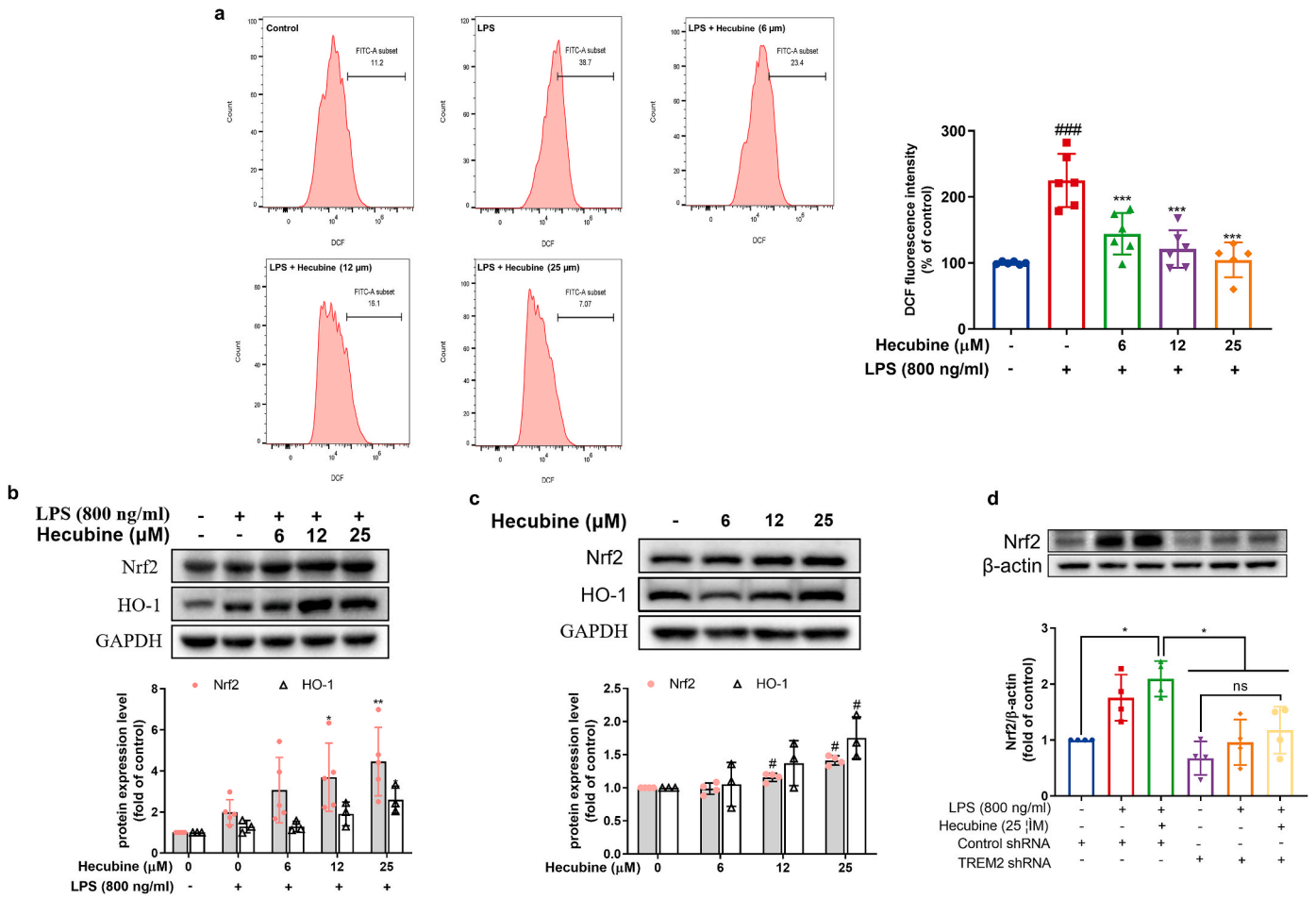

Fig. 7. Hecubine suppressed ROS production but activated Nrf2 and HO-1 expression. Cells were pretreated with Hecubine for 1 h and then stimulated with/without LPS. (a) The ROS production was determined using flow cytometry analysis (n = 5–6). (b–c) The protein levels of Nrf2 (b, n = 5; c, n = 4) and HO-1 (b, n = 3; c, n = 3) were measured via Western blotting. (d) Cells were transfected with negative control shRNA or TREM2 shRNA. Nrf2 expression level in BV2 cells after treatment with Hecubine or LPS was assessed by Western blot analysis (n = 4). Quantitative analysis was carried out using ImageJ. – and + represent the absence and presence of LPS (800 ng/ml), respectively. The data are presented as the mean ± SD of at least three independent experiments. *$p < 0.05$, **$p < 0.01$, and ***$p < 0.001$ vs. LPS-treated group; ###$p < 0.001$ vs. control; ns, not significant; One-way ANOVA with Dunnett's multiple comparisons test.

Hecubine on pro-inflammatory cytokine expression in the LPS-stimulated zebrafish larvae model. Hecubine incubation significantly reversed the tendency to upregulated the expression of pro-inflammatory mediators and cytokines, including iNOS, TNF-α, IL-6, and IL-1β, in an *in vivo* neuroinflammation model (Fig. 9f–h).

3.9. *Hecubine exhibited anti-inflammation and antioxidation via activation of TREM2 and Nrf2 expression in the LPS-stimulated zebrafish larvae model*

Fluorescence images demonstrated that the level of ROS was increased by ~50 % after exposure to LPS. Pretreatment with Hecubine (12 and 25 μM) reduced the ROS accumulation induced by LPS in zebrafish larvae (Fig. 10a and b). Additionally, we investigated the role of Hecubine in TREM2-mediated anti-inflammation and Nrf2-mediated antioxidant pathways. The Western blot results showed increased expression of TREM2, Nrf2, and HO-1 upon treatment with Hecubine in the LPS-stimulated zebrafish larvae model. Specifically, 25 μM of Hecubine led to a ~2-fold increase in Nrf2 expression in zebrafish larvae (Fig. 10c and d).

4. Discussion

Based on data from the World Health Organization (WHO), an estimated 35 million individuals are suffering from drug abuse, with approximately 0.5 million deaths attributed to drug addiction each year. In addition, it is projected that the number of patients with neurodegenerative diseases will exceed 70 million by 2030 [32]. The modulation of immune responses has emerged as a promising therapeutic approach for treating inflammation-associated neurological disorders [33]. TREM2 has gained increasing attention due to its significant role in the regulation of neuroinflammation, and its activation has been demonstrated to suppress abnormal activation of microglia, thereby exerting a neuroprotective effect [34]. In this study, we identified Hecubine, a natural small-molecule MIA derived from *E. officinalis*, as a potential TREM2 activator and investigated its mechanism of action in alleviating lipopolysaccharide (LPS)-induced neuroinflammation both *in vitro* and *in vivo*.

Excessive nitric oxide (NO) reacts with oxygen-free radicals, leading to the formation of harmful oxidative compounds, resulting in an inflammatory response, oxidative stress, and cell damage [35]. In recent years, NO production has been commonly used to assess the anti-inflammatory properties of MIAs in *E. officinalis*. For example, Zhang M et al. reported that the IC_{50} values of two newly discovered iboga-type alkaloids were 10.6 and 13.5 μM, respectively, for the inhibition of LPS-induced NO production in RAW 264.7 macrophage cells [36]. Similarly, Zhao X et al. found that two novel aspidosperma-type alkaloids exhibited anti-inflammatory activity with IC_{50} values of 14.5

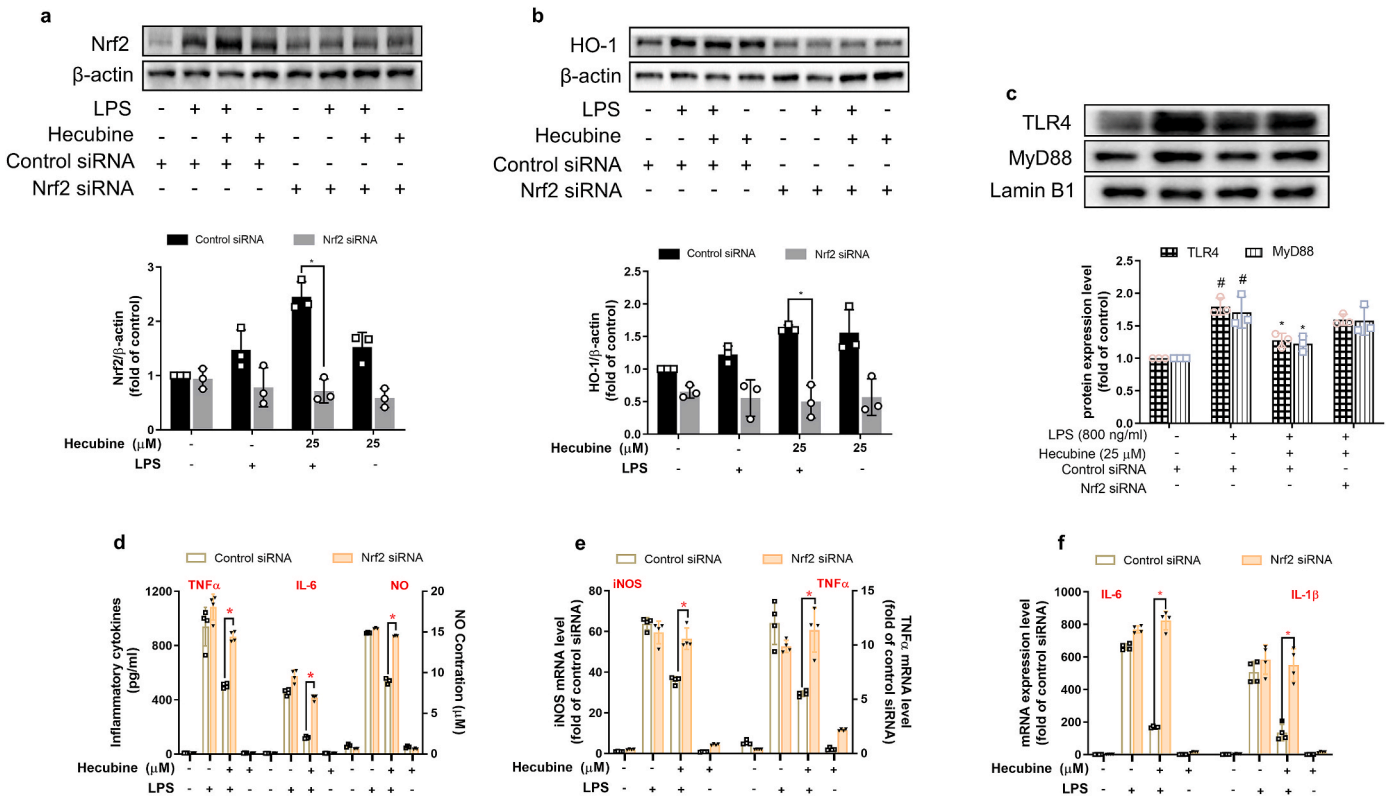

Fig. 8. Blockade of Nrf2 abolished the anti-inflammatory effect of Hecubine. BV2 cells were treated with Hecubine in the presence or absence of LPS after transient transfection of Nrf2 siRNA and control siRNA. The protein levels of Nrf2 (a), HO-1 (b), TLR4, and MyD88 (c) were determined by Western blotting (n = 3). The production of TNF-α, IL-6, and NO (d) was measured via Griess reagent and an ELISA assay, respectively (n = 3). The mRNA levels of iNOS, TNF-α (e), IL-6, and IL-1β (f) were detected by qPCR analysis (n = 4). The data from the experiments are expressed as the mean ± SD of three independent experiments. *$p < 0.05$ vs. LPS-treated group; #$p < 0.05$ vs. control; One-way ANOVA with Dunnett's multiple comparisons test.

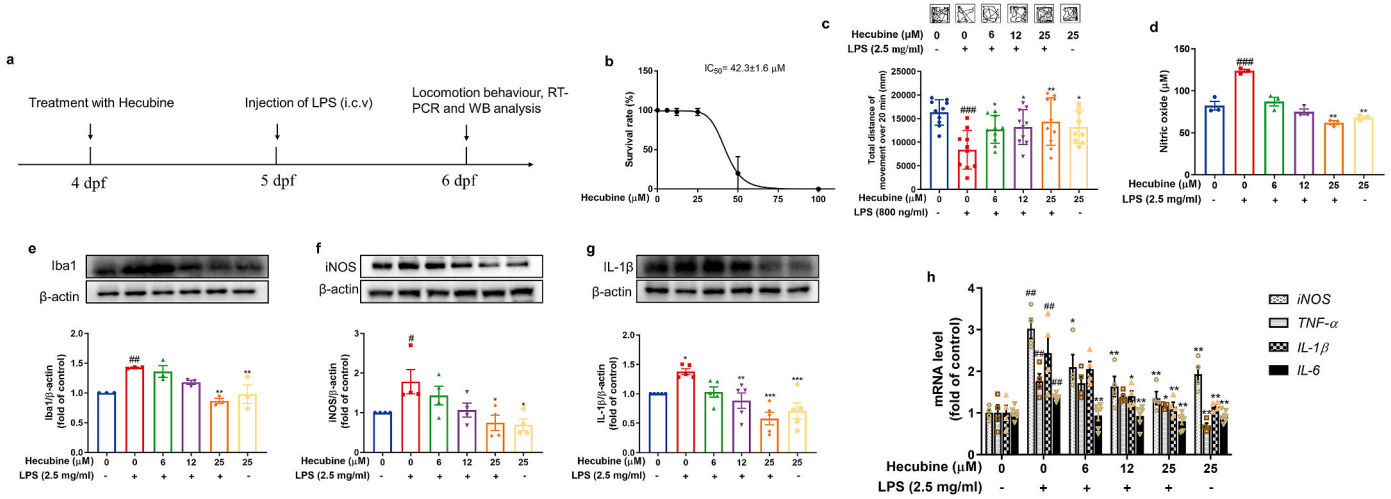

Fig. 9. Hecubine modulated locomotor deficits and exhibited anti-inflammatory activity in LPS-stimulated zebrafish larvae. (a) Schematic of compound administration in zebrafish. (b) Toxicity of Hecubine in the zebrafish model (n = 12 zebrafish per group). (c) Representative patterns of behavioral locomotion in zebrafish larvae and quantitative analysis of zebrafish locomotion in the control and treated groups (n = 9~10 zebrafish per group). (d) Production of NO measured by Griess assay (n = 3). (e–g) Protein expression of Ibal (n = 3) (e), iNOS (Kruskal-Wallis test of One-way ANOVA, n = 4) (f), and IL-1β (n = 5) (g) was quantified by Western Blot. (h) The mRNA expression levels of TNF-α, IL-1β, and IL-6 were analyzed by qPCR, n ≥ 4. The data are mean ± SEM. *$p < 0.05$ and **$p < 0.01$ vs. LPS-treated group; ###$p < 0.001$ vs. control; One-way ANOVA with Dunnett's multiple comparisons test.

and 22.1 μM, respectively, in RAW 264.7 macrophage cells [37]. In our study, Hecubine and its analogue MIAs significantly reduced LPS-induced NO production at different doses. The IC_{50} of Hecubine was approximately 6 μM, surpassing the efficacy of the aforementioned compounds. Furthermore, our structure-activity relationship analysis suggests that the presence of a 14,15-epoxy group in the structure of Hecubine may contribute to its improved anti-inflammatory activity and reduced cytotoxicity compared to a hydroxyl group at positions 14 and 15. Additionally, the toxicity results from zebrafish experiments indicated that compounds **2** and **7**, consistent with cytotoxicity, exhibited

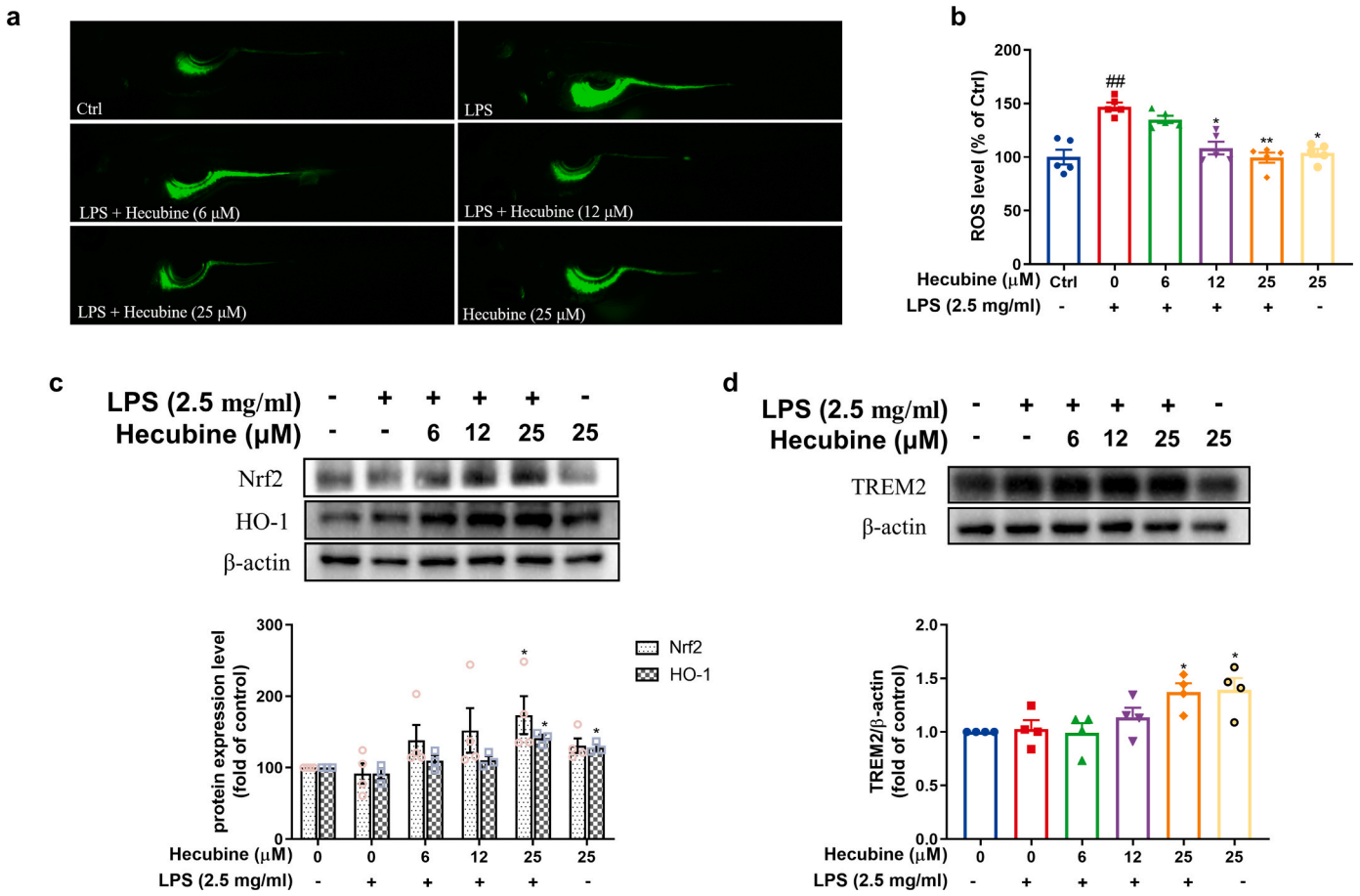

Fig. 10. Hecubine exhibited an antioxidative effect in LPS-stimulated zebrafish larvae. Zebrafish larvae were treated as described above. (a) ROS levels were measured by image analysis and fluorescence microscopy; Kruskal-Wallis test of One-way ANOVA (n = 5). (b) Fluorescence intensity was quantified using ImageJ. The protein levels of Nrf2 (n = 4), HO-1 (n = 3) (c), and TREM2 (n = 4) (d) were assessed by Western Blot. The data are the mean ± SEM of at least three independent experiments. *$p < 0.05$, **$p < 0.01$, and ***$p < 0.001$ vs. LPS-treated group; ###$p < 0.001$ vs. control; One-way ANOVA with Dunnett's multiple comparisons test.

the highest toxicity towards zebrafish growth and development (Fig. S8). This suggests that the presence of a methyl ester group at position 16 may enhance the biological toxicity of MIAs. Moreover, the hydroxyl group at position 16 and the methyl group at position 1 also play a role in reducing cytotoxicity. Importantly, none of the tested compounds induced pericardial edema or cardiac malformations, while zebrafish larvae treated with 100 μM ibogaine reportedly experienced yolk sac and/or pericardial edemas [38]. These findings provide insight into the chemical structure determinant of these iboga analogues that could contribute to potential cardiotoxicity and offer clues for further structural modification to increase efficacy and lower cardiac toxicity. To summarize, the structure-activity relationship of Hecubine and its analogues provides insights into how to improve efficacy and reduce side effects by modifying the structures of these compounds as future work.

As an important microglial surface receptor, TREM2 interacts with the transduction partner DAP12 to regulate neuroinflammation in the CNS [39]. The role of TREM2 in neuroinflammation and inflammation-related neurodegenerative diseases remains somewhat controversial. However, it is widely recognized that the activation and enhancement of TREM2 in the early stages of neurodegenerative diseases can protect neuronal cells and improve disease progression [40]. For example, in Parkinson's disease (PD), α-synuclein can be recognized by TREM2, leading to the activation of TREM2, which promotes microglial phagocytosis and degradation of α-synuclein [41]. On the other hand, abnormal TREM2 function can lead to an imbalance in the immune response and worsen the symptoms of inflammation-related neurodegenerative diseases. Knockdown of TREM2 in 5xFAD mice, for instance, has been shown to significantly elevate the levels of pro-inflammatory cytokines, such as IL-1β and TNF-α, subsequently causing impairment of amyloid engulfment and aggravated cognitive deficits in the mice [42]. Additionally, mutations in TREM2 and its co-receptor DAP12, including the p.R47H mutation in TREM2, accelerate the risk of the development of Nasu-Hakola disease, AD, and PD [6,41]. Therefore, targeting TREM2 has emerged as a potential therapeutic approach for neuroinflammatory diseases. In the present study, we discovered Hecubine has the capability to directly bind to and activate TREM2, leading to a significant inhibition of LPS-induced neuroinflammation in BV2 microglial cells. Knockdown of TREM2 reversed the inhibitory effects of Hecubine on the release of pro-inflammatory cytokines.

Previous studies have shown that overexpression of TREM2 suppresses TLR4 activation and its downstream pro-inflammatory pathways, resulting in the inhibition of pro-inflammatory cytokine production [43]. Therefore, we evaluated whether Hecubine could inhibit TLR4 expression by targeting TREM2. Our results showed that TREM2 silencing eliminated the blocking effect of Hecubine on TLR4 expression. TLR4, a crucial pattern recognition receptor, mediates the innate and adaptive immunological inflammatory response processes associated with drug addiction [44]. Studies have shown that TLR4 in the spinal cord or periaqueductal gray mediates neuroinflammation and tolerance following persistent morphine therapy, while systemic knockout of TLR4 suppresses morphine reward [45,46]. In our experiment, Hecubine significantly suppressed the activation of TLR4 and

expression of MyD88 in LPS-treated BV-2 microglia cells, suggesting that Hecubine may have potential as an anti-addictive agent; this merits further investigation. Furthermore, Hecubine obviously activated TREM2 expression and inhibited various downstream signal pathways of TLR4 signaling, such as the MAPK, PI3K/Akt, Nrf2, and NF-κB pathways, thereby attenuating oxidative stress and inflammation. Therefore, we speculated that Hecubine may target TREM2 to regulate the LPS-induced imbalance between microglial TREM2 and TLR4, ultimately inhibiting neuroinflammatory responses in LPS-activated BV-2 microglial cells.

We further investigated the mechanisms underlying the antioxidant properties of Hecubine in microglia and zebrafish. Excessive oxidative stress, characterized by overproduction of intracellular levels of reactive oxygen species (ROS), exacerbates the development of neuroinflammatory diseases [47]. The activation of cellular stress responses, such as the heat shock response, plays a crucial role in combating oxidative stress and inflammation. This response involves the regulation of cytoprotective vitagene genes, which produce molecules endowed with antioxidant and anti-apoptotic activity [48]. Nrf2-mediated HO-1 is an important component of the vitagene network [11]. Under normal conditions, Nrf2 is sequestered in the cytoplasm by a protein called Kelch-like ECH-associated protein 1 (Keap-1). However, when cells experience oxidative stress, Nrf2 is released from Keap-1 and translocates into the cell nucleus. Once in the nucleus, Nrf2 binds to antioxidant response elements (AREs) in the DNA, initiating the transcription of cytoprotective genes such as HO-1 [49]. Upregulation of Nrf2 and HO-1 signaling provides protection against various electrophiles and oxidants, which are involved in the pathogenesis of neurodegeneration and aging [11]. Furthermore, the upregulation of HO-1 results in an elevation in bilirubin production, which possesses antioxidative and neurotrophin-like properties [50]. Here, we discovered that Hecubine significantly reduced ROS production in microglia cells and zebrafish larvae by activating the Nrf2/HO-1 signaling pathway. Blockade of Nrf2 activity using siRNA also inhibited HO-1 expression. Moreover, Nrf2 has been shown to exert not only anti-oxidative effects but also regulate the neuroinflammatory response in microglia [51]. Previous research demonstrated that Nrf2-knockout mice were hypersensitive to LPS-induced inflammation [52]. In our study, the inhibition of LPS-induced pro-inflammatory mediators and cytokines by Hecubine was reversed by Nrf2 siRNA transfection, indicating that Hecubine alleviated LPS-induced neuroinflammatory responses in the CNS via the activation of Nrf2.

The intricate crosstalk among the TREM2, TLR4, and Nrf2 pathways is thought to intricately influence the progression of the inflammatory response. Emerging evidence indicates Nrf2 expression is increased by overexpressing TREM2 and decreased by downregulating TREM2 in BV2 cells. Nrf2, in turn, may regulate the initiation of TREM2, thereby mediating the microglial anti-inflammatory phenotype [15]. Our study has confirmed that knockdown of TREM2 abolished the anti-inflammatory effect of Hecubine by decreasing Nrf2 expression in LPS-stimulated BV2 cells. However, it's worth noting that TREM2 shRNA has not completely prevented Hecubine-induced Nrf2 upregulation, suggesting Hecubine may have additional sites of action beyond TREM2 to exert its antioxidant effects. Furthermore, activation of the Nrf2 pathway by TLR agonists can promote antioxidant molecule production, thereby improving cell survival. Conversely, Nrf2 activation can suppress pro-inflammatory mediators to inhibit TLR-mediated excessive inflammation [53]. The crosstalk between Nrf2 and TLR4 may also be engendered by interactions of the former with the NF-κB pathway. Briefly, p65 may facilitate the nuclear transport of Keap1 and compete with Nrf2 for binding to the transcriptional coactivator CREB-binding protein-p300 complex (CBP) to down-regulate the Nrf2 pathway [54]. Although there is limited evidence that TLR4 directly regulates Nrf2 activation, research has shown that MyD88 signaling promotes Nrf2 in response to LPS-induced inflammation [55]. In the current study, Nrf2 silencing also reduced Hecubine-induced inhibitory effects on TLR4 and MyD88 expression, suggesting that Nrf2 may participate in the inflammatory response by regulating TLR4/MyD88 signaling pathways. However, further research is required to elucidate the more in-depth underlying mechanisms.

Zebrafish (Danio rerio) are commonly utilized as an *in vivo* model to assess toxicity and inflammation due to their abundance, cost-effectiveness, and similarities to humans in terms of phagocytic processes and inflammatory factors [56]. In our *in vivo* experiments, Hecubine administration resulted in a remarkable alleviation of neuroinflammatory symptoms using a zebrafish model of LPS-induced neuroinflammation. Treatment with Hecubine in zebrafish larvae resulted in a significant improvement of locomotion behavior deficits and a reduction of neuroinflammation, achieved through the activation of TREM2 and subsequent downstream Nrf2 signaling pathways. Moreover, accumulating evidence demonstrates that microglia are present in the zebrafish brain and establish the initial blood-brain barrier (BBB) around 2.5 dpf [57,58]. Given that Hecubine suppressed LPS-induced microglia activation and exhibited anti-neuroinflammatory activities in 4 dpf larvae, it is possible that Hecubine can penetrate the BBB to exert its effect. However, further investigations are warranted to delve into this aspect and elucidate the precise mechanism by which Hecubine crosses the blood-brain barrier in zebrafish larvae, thus providing additional insights into its therapeutic potential.

5. Conclusions

This study presents the first evidence that Hecubine acts as a promising and new TREM2 activator with potential therapeutic implications for alleviating lipopolysaccharide (LPS)-induced neuroinflammation both *in vitro* and *in vivo*. In BV2 microglial cells, Hecubine directly targeted TREM2 to block LPS-induced secretion of proinflammatory mediators (NO, PEG_2, and ROS) and the production of proinflammatory cytokines (TNF-α, IL-1β, and IL-6) via regulating TLR4/MyD88/MAPK/NF-κB and Nrf2/HO-1 signaling pathways. In zebrafish, Hecubine activated the TREM2 and Nrf2 pathways, leading to the alleviation of LPS-induced swimming deficits, oxidative stress, and inflammatory responses. This study strongly suggests that Hecubine has the potential to prevent neuroinflammatory responses and reduce oxidative stress, making it a promising candidate for the treatment of diseases associated with neural inflammation.

Funding

This work was supported by the Science and Technology Development Fund (FDCT) of Macao SAR (No.: 0058/2019/A1 and 0016/2019/AKP), University of Macau (No.: MYRG2019-00159-ICMS, MYRG2020-00183-ICMS, MYRG2022-00263-ICMS, and CPG2022-00023-ICMS), Shenzhen-Hong Kong-Macao Science and Technology Innovation Project (Category C) of Shenzhen Science and Technology Innovation Committee (No.: EF038/ICMS-LMY/2021/SZSTIC), and National Natural Science Foundation for Young Scientists of China (No. 81803398).

Ethics statement

All experimental procedures were according to the guidelines of Regulations of Experimental Animal Administration issued by the State Committee of Science and Technology of the People's Republic of China, and were approved by the Animal Research Ethics Committee of the University of Macau, China (permit number: UMARE-021b-2020).

CRediT authorship contribution statement

Lin Li: Conceptualization, Data curation, Formal analysis, Investigation, Methodology, Project administration, Software, Validation, Visualization, Writing – original draft, Writing – review & editing. **Yu-Lin He:** Conceptualization, Data curation, Formal analysis,

Investigation, Methodology, Validation, Visualization, Writing – review & editing. **Nan Xu:** Data curation, Formal analysis, Investigation, Methodology, Software, Validation, Visualization, Writing – review & editing. **Xiu-Fen Wang:** Conceptualization, Data curation, Validation, Writing – original draft, Writing – review & editing. **Bing Song:** Conceptualization, Data curation, Methodology, Project administration, Supervision, Writing – original draft, Writing – review & editing. **Ben-Qin Tang:** Conceptualization, Data curation, Formal analysis, Funding acquisition, Investigation, Methodology, Project administration, Resources, Supervision, Writing – original draft, Writing – review & editing. **Simon Ming-Yuen Lee:** Conceptualization, Data curation, Formal analysis, Funding acquisition, Investigation, Methodology, Project administration, Resources, Software, Supervision, Validation, Visualization, Writing – original draft, Writing – review & editing.

Declaration of competing interest

The authors declare that they have no known competing financial interests or personal relationships that could have appeared to influence the work reported in this paper.

Data availability

Data will be made available on request.

Appendix A. Supplementary data

Supplementary data to this article can be found online at https://doi.org/10.1016/j.redox.2024.103057.

References

[1] R. Brambilla, Neuroinflammation, the thread connecting neurological disease, Acta Neuropathol. 137 (5) (2019) 689–691.

[2] J. Cuitavi, J.V. Torres-Pérez, J.D. Lorente, Y. Campos-Jurado, P. Andrés-Herrera, A. Polache, C. Agustín-Pavón, L. Hipólito, Crosstalk between Mu-Opioid receptors and neuroinflammation: consequences for drug addiction and pain, Neurosci. Biobehav. Rev. (2022) 105011.

[3] C.K. Glass, K. Saijo, B. Winner, M.C. Marchetto, F.H. Gage, Mechanisms underlying inflammation in neurodegeneration, Cell 140 (6) (2010) 918–934.

[4] P. Zhao, Y. Xu, L.-L. Jiang, X. Fan, Z. Ku, L. Li, X. Liu, M. Deng, H. Arase, J.-J. Zhu, LILRB2-mediated TREM2 signaling inhibition suppresses microglia functions, Mol. Neurodegener. 17 (1) (2022) 44.

[5] M.H. Ri, Y. Xing, H.X. Zuo, M.Y. Li, H.L. Jin, J. Ma, X. Jin, Regulatory mechanisms of natural compounds from traditional Chinese herbal medicines on the microglial response in ischemic stroke, Phytomedicine (2023) 154889.

[6] M.M. Painter, Y. Atagi, C.-C. Liu, R. Rademakers, H. Xu, J.D. Fryer, G. Bu, TREM2 in CNS homeostasis and neurodegenerative disease, Mol. Neurodegener. 10 (2015) 1–10.

[7] S. Chen, J. Peng, P. Sherchan, Y. Ma, S. Xiang, F. Yan, H. Zhao, Y. Jiang, N. Wang, J.H. Zhang, TREM2 activation attenuates neuroinflammation and neuronal apoptosis via PI3K/Akt pathway after intracerebral hemorrhage in mice, J. Neuroinflammation 17 (1) (2020) 1–16.

[8] S. Wang, R. Sudan, V. Peng, Y. Zhou, S. Du, C.M. Yuede, T. Lei, J. Hou, Z. Cai, M. Cella, TREM2 drives microglia response to amyloid-β via SYK-dependent and-independent pathways, Cell 185 (22) (2022) 4153–4169.

[9] H. Wang, X. Li, Q. Wang, J. Ma, X. Gao, M. Wang, TREM2, microglial and ischemic stroke, J. Neuroimmunol. (2023) 578108.

[10] V. Calabrese, J. Giordano, A. Signorile, M. Laura Ontario, S. Castorina, C. De Pasquale, G. Eckert, E.J. Calabrese, Major pathogenic mechanisms in vascular dementia: roles of cellular stress response and hormesis in neuroprotection, J. Neurosci. Res. 94 (12) (2016) 1588–1603.

[11] V. Calabrese, C. Cornelius, A.T. Dinkova-Kostova, E.J. Calabrese, M.P. Mattson, Cellular stress responses, the hormesis paradigm, and vitagenes: novel targets for therapeutic intervention in neurodegenerative disorders, Antioxidants Redox Signal. 13 (11) (2010) 1763–1811.

[12] S. Jin, X. Wang, X. Xiang, Y. Wu, J. Hu, Y. Li, Y.L. Dong, Y. Tan, X. Wu, Inhibition of GPR17 with cangrelor improves cognitive impairment and synaptic deficits induced by Aβ1–42 through Nrf2/HO-1 and NF-κB signaling pathway in mice, Int. Immunopharm. 101 (2021) 108335.

[13] P. Gervois, I. Lambrichts, The emerging role of triggering receptor expressed on myeloid cells 2 as a target for immunomodulation in ischemic stroke, Front. Immunol. 10 (2019) 1668.

[14] S. Liu, X. Cao, Z. Wu, S. Deng, H. Fu, Y. Wang, F. Liu, TREM2 improves neurological dysfunction and attenuates neuroinflammation, TLR signaling and neuronal apoptosis in the acute phase of intracerebral hemorrhage, Front. Aging Neurosci. 14 (2022) 967825.

[15] L. He, Y. Zheng, L. Huang, J. Ye, Y. Ye, H. Luo, X. Chen, W. Yao, J. Chen, J.-c. Zhang, Nrf2 regulates the arginase 1+ microglia phenotype through the initiation of TREM2 transcription, ameliorating depression-like behavior in mice, Transl. Psychiatry 12 (1) (2022) 459.

[16] Q. Pan, N.R. Mustafa, K. Tang, Y.H. Choi, R. Verpoorte, Monoterpenoid indole alkaloids biosynthesis and its regulation in Catharanthus roseus: a literature review from genes to metabolites, Phytochemistry Rev. 15 (2) (2016) 221–250.

[17] A.E. Mohammed, Z.H. Abdul-Hameed, M.O. Alotaibi, N.O. Bawakid, T.R. Sobahi, A. Abdel-Lateff, W.M. Alarif, Chemical diversity and bioactivities of monoterpene indole alkaloids (MIAs) from six Apocynaceae genera, Molecules 26 (2) (2021) 488.

[18] D.-B. Zhang, D.-G. Yu, M. Sun, X.-X. Zhu, X.-J. Yao, S.-Y. Zhou, J.-J. Chen, K. Gao, Ervatamines A–I, anti-inflammatory monoterpenoid indole alkaloids with diverse skeletons from Ervatamia hainanensis, J. Nat. Prod. 78 (6) (2015) 1253–1261.

[19] K.R. Alper, H.S. Lotsof, C.D. Kaplan, The ibogaine medical subculture, J. Ethnopharmacol. 115 (1) (2008) 9–24.

[20] T. Knuijver, A. Schellekens, M. Belgers, R. Donders, T. van Oosteren, K. Kramers, R. Verkes, Safety of ibogaine administration in detoxification of opioid-dependent individuals: a descriptive open-label observational study, Addiction 117 (1) (2022) 118–128.

[21] D.C. Mash, L. Duque, B. Page, K. Allen-Ferdinand, Ibogaine detoxification transitions opioid and cocaine abusers between dependence and abstinence: clinical observations and treatment outcomes, Front. Pharmacol. 9 (2018) 529.

[22] Y. Yu, S.-M. Zhao, M.-F. Bao, X.-H. Cai, An Aspidosperma-type alkaloid dimer from Tabernaemontana bovina as a candidate for the inhibition of microglial activation, Org. Chem. Front. 7 (11) (2020) 1365–1373.

[23] C. Gomez Gonzalez, J. Martinez, Phytochemistry of Ervatamia coronaria Stapf.(II). Hecubine and voaphylline: two alkaloids present in leaves, Rev. Cubana Farmac. 10 (1976) 45–54.

[24] C.M. Naidoo, Y. Naidoo, Y.H. Dewir, H.N. Murthy, S. El-Hendawy, N. Al-Suhaibani, Major bioactive alkaloids and biological activities of Tabernaemontana species (Apocynaceae), Plants 10 (2) (2021) 313.

[25] M. Westerfield, The Zebrafish Book: a Guide for the Laboratory Use of Zebrafish, 2000. http://zfin.org/zf_info/zfbook/zfbk.html.

[26] Y. Wang, Z. Fan, M. Yang, Y. Wang, J. Cao, A. Khan, Y. Liu, G. Cheng, Protective effects of E Se tea extracts against alcoholic fatty liver disease induced by high fat/alcohol diet: in vivo biological evaluation and molecular docking study, Phytomedicine 101 (2022) 154113.

[27] R. Zeng, Y. Chen, S. Zhao, G.-h. Cui, Autophagy counteracts apoptosis in human multiple myeloma cells exposed to oridonin in vitro via regulating intracellular ROS and SIRT1, Acta Pharmacol. Sin. 33 (1) (2012) 91–100.

[28] C. Lv, Y. Huang, Q. Wang, C. Wang, H. Hu, H. Zhang, D. Lu, H. Jiang, R. Shen, W. Zhang, Ainsliadimer A induces ROS-mediated apoptosis in colorectal cancer cells via directly targeting peroxiredoxin 1 and 2, Cell Chem. Biol. 30 (3) (2023) 295–307.

[29] J. Zhou, W. Yu, M. Zhang, X. Tian, Y. Li, Y. Lü, Imbalance of microglial TLR4/TREM2 in LPS-treated APP/PS1 transgenic mice: a potential link between Alzheimer's disease and systemic inflammation, Neurochem. Res. 44 (2019) 1138–1151.

[30] Q. Huang, L. Zhan, H. Cao, J. Li, Y. Lyu, X. Guo, J. Zhang, L. Ji, T. Ren, J. An, Increased mitochondrial fission promotes autophagy and hepatocellular carcinoma cell survival through the ROS-modulated coordinated regulation of the NFKB and TP53 pathways, Autophagy 12 (6) (2016) 999–1014.

[31] Y. He, S.M.Y. Lee, Brain ventricular microinjections of lipopolysaccharide into larval zebrafish to assess neuroinflammation and neurotoxicity, JoVE (186) (2022) e64313.

[32] O. World Health, Dementia: a Public Health Priority, World Health Organization, 2012.

[33] A. Cippitelli, E. Domi, M. Ubaldi, J.C. Douglas, H.W. Li, G. Demopulos, G. Gaitanaris, M. Roberto, P.D. Drew, C.J.M. Kane, Protection against alcohol-induced neuronal and cognitive damage by the PPARγ receptor agonist pioglitazone, Brain Behav. Immun. 64 (2017) 320–329.

[34] A.A. Nugent, K. Lin, B. Van Lengerich, S. Lianoglou, L. Przybyla, S.S. Davis, C. Llapashtica, J. Wang, D. Xia, A. Lucas, TREM2 regulates microglial cholesterol metabolism upon chronic phagocytic challenge, Neuron 105 (5) (2020) 837–854.

[35] V. Calabrese, C. Mancuso, M. Calvani, E. Rizzarelli, D.A. Butterfield, A.M. Giuffrida Stella, Nitric oxide in the central nervous system: neuroprotection versus neurotoxicity, Nat. Rev. Neurosci. 8 (10) (2007) 766–775.

[36] M. Zhang, S.-Y. Du, J. Liu, X. Zhao, J.-N. Liu, C.-S. Jiang, K.-K. Zhu, L. Fang, New monoterpenoid indole alkaloids from Tabernaemontana bovina, Phytochem. Lett. 43 (2021) 23–26.

[37] X. Zhao, S.-Y. Du, J. Liu, J.-N. Liu, C.-S. Jiang, K.-K. Zhu, L. Fang, New aspidosperma-type alkaloids from Tabernaemontana bovina, Phytochem. Lett. 49 (2022) 105–108.

[38] L.P. Cameron, R.J. Tombari, J. Lu, A.J. Pell, Z.Q. Hurley, Y. Ehinger, M.V. Vargas, M.N. McCarroll, J.C. Taylor, D. Myers-Turnbull, A non-hallucinogenic psychedelic analogue with therapeutic potential, Nature 589 (7842) (2021) 474–479.

[39] Y. Zhou, M. Tada, Z. Cai, P.S. Andhey, A. Swain, K.R. Miller, S. Gilfillan, M. N. Artyomov, M. Takao, A. Kakita, Human early-onset dementia caused by DAP12 deficiency reveals a unique signature of dysregulated microglia, Nat. Immunol. 24 (3) (2023) 545–557.

[40] T.R. Jay, V.E. von Saucken, G.E. Landreth, TREM2 in neurodegenerative diseases, Mol. Neurodegener. 12 (1) (2017) 1–33.

[41] X.-x. Li, F. Zhang, Targeting TREM2 for Parkinson's disease: where to go? Front. Immunol. 12 (2021) 795036.
[42] Y. Wang, Y. Lin, L. Wang, H. Zhan, X. Luo, Y. Zeng, W. Wu, X. Zhang, F. Wang, TREM2 ameliorates neuroinflammatory response and cognitive impairment via PI3K/AKT/FoxO3a signaling pathway in Alzheimer's disease mice, Aging (Albany NY) 12 (20) (2020) 20862.
[43] M.J. Perugorria, A. Esparza-Baquer, F. Oakley, I. Labiano, A. Korosec, A. Jais, J. Mann, D. Tiniakos, A. Santos-Laso, A. Arbelaiz, Non-parenchymal TREM-2 protects the liver from immune-mediated hepatocellular damage, Gut 68 (3) (2019) 533–546.
[44] J.M. Green, M.H. Sundman, Y.-H. Chou, Opioid-induced microglia reactivity modulates opioid reward, analgesia, and behavior, Neurosci. Biobehav. Rev. 135 (2022) 104544.
[45] L.N. Eidson, K. Inoue, L.J. Young, M.G. Tansey, A.Z. Murphy, Toll-like receptor 4 mediates morphine-induced neuroinflammation and tolerance via soluble tumor necrosis factor signaling, Neuropsychopharmacology 42 (3) (2017) 661–670.
[46] H. Wang, M. Huang, W. Wang, Y. Zhang, X. Ma, L. Luo, X. Xu, L. Xu, H. Shi, Y. Xu, Microglial TLR4-induced TAK1 phosphorylation and NLRP3 activation mediates neuroinflammation and contributes to chronic morphine-induced antinociceptive tolerance, Pharmacol. Res. 165 (2021) 105482.
[47] Y. Kuthati, P. Busa, S. Tummala, V.N. Rao, V.N.G. Davuluri, Y.-P. Ho, C.-S. Wong, Mesoporous polydopamine nanoparticles attenuate morphine tolerance in neuropathic pain rats by inhibition of oxidative stress and restoration of the endogenous antioxidant system, Antioxidants 10 (2) (2021) 195.
[48] M. Concetta Scuto, C. Mancuso, B. Tomasello, M. Laura Ontario, A. Cavallaro, F. Frasca, L. Maiolino, A. Trovato Salinaro, E.J. Calabrese, V. Calabrese, Curcumin, hormesis and the nervous system, Nutrients 11 (10) (2019) 2417.
[49] W. Chauhan, R. Zennadi, Keap1-Nrf2 heterodimer: a therapeutic target to ameliorate sickle cell disease, Antioxidants 12 (3) (2023) 740.
[50] C. Mancuso, C. Capone, S.C. Ranieri, S. Fusco, V. Calabrese, M.L. Eboli, P. Preziosi, T. Galeotti, G. Pani, Bilirubin as an endogenous modulator of neurotrophin redox signaling, J. Neurosci. Res. 86 (10) (2008) 2235–2249.
[51] W. Tao, Y. Hu, Z. Chen, Y. Dai, Y. Hu, M. Qi, Magnolol attenuates depressive-like behaviors by polarizing microglia towards the M2 phenotype through the regulation of Nrf2/HO-1/NLRP3 signaling pathway, Phytomedicine 91 (2021) 153692.
[52] R. Dhar, M.N. Rana, L. Zhang, Y. Li, N. Li, Z. Hu, C. Yan, X. Wang, X. Zheng, H. Liu, Phosphodiesterase 4B is required for NLRP3 inflammasome activation by positive feedback with Nrf2 in the early phase of LPS-induced acute lung injury, Free Radic. Biol. Med. 176 (2021) 378–391.
[53] J. Muri, H. Wolleb, P. Broz, E.M. Carreira, M. Kopf, Electrophilic Nrf2 activators and itaconate inhibit inflammation at low dose and promote IL-1β production and inflammatory apoptosis at high dose, Redox Biol. 36 (2020) 101647.
[54] S. Rius-Pérez, S. Pérez, P. Martí-Andrés, M. Monsalve, J. Sastre, Nuclear factor kappa B signaling complexes in acute inflammation, Antioxidants Redox Signal. 33 (3) (2020) 145–165.
[55] K.H. Kim, J.H. Lyu, S.T. Koo, S.-R. Oh, H.-K. Lee, K.-S. Ahn, R.T. Sadikot, M. Joo, MyD88 is a mediator for the activation of Nrf2, Biochem. Biophys. Res. Commun. 404 (1) (2011) 46–51.
[56] N. Kyritsis, C. Kizil, S. Zocher, V. Kroehne, J. Kaslin, D. Freudenreich, A. Iltzsche, M. Brand, Acute inflammation initiates the regenerative response in the adult zebrafish brain, Science 338 (6112) (2012) 1353–1356.
[57] J. Xu, T. Wang, Y. Wu, W. Jin, Z. Wen, Microglia colonization of developing zebrafish midbrain is promoted by apoptotic neuron and lysophosphatidylcholine, Dev. Cell 38 (2) (2016) 214–222.
[58] Z. Yang, P. Lin, B. Chen, X. Zhang, W. Xiao, S. Wu, C. Huang, D. Feng, W. Zhang, J. Zhang, Autophagy alleviates hypoxia-induced blood-brain barrier injury via regulation of CLDN5 (claudin 5), Autophagy 17 (10) (2021) 3048–3067.